

NIST Special Publication 250-83
Revision 1

Calibration of Hygrometers with the Hybrid Humidity Generator

C. W. Meyer

T. Herman

W. W. Miller

Thermodynamic Metrology Group

Sensor Science Division

Physical Measurement Laboratory

This publication is available free of charge from:
<https://doi.org/10.6028/NIST.SP.250-83r1>

September 2021



U.S. Department of Commerce
Gina M. Raimondo, Secretary

National Institute of Standards and Technology
*James K. Olthoff, Performing the Non-Exclusive Functions and Duties of the Under Secretary of Commerce
for Standards and Technology & Director, National Institute of Standards and Technology*

Certain commercial entities, equipment, or materials may be identified in this document in order to describe an experimental procedure or concept adequately. Such identification is not intended to imply recommendation or endorsement by the National Institute of Standards and Technology, nor is it intended to imply that the entities, materials, or equipment are necessarily the best available for the purpose.

National Institute of Standards and Technology Special Publication SP 250-83 Revision 1
Natl. Inst. Stand. Technol. Spec. Publ. 250-83 Rev. 1, 75 pages (September 2021)
CODEN: NSPUE2

This publication is available free of charge from:
<https://doi.org/10.6028/NIST.SP.250-83r1>

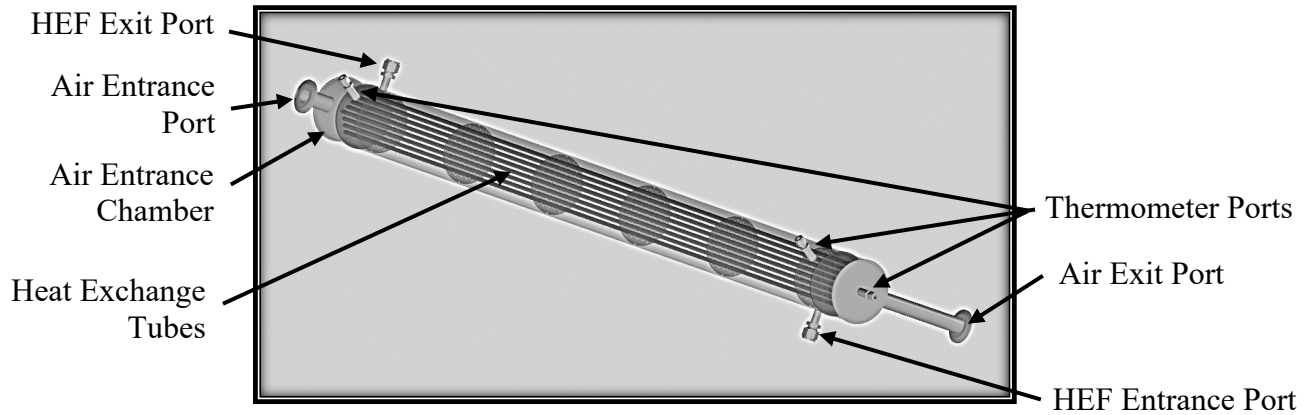
passing through the hole, the air is immediately directed radially outward by a diffuser plate of diameter 15.2 cm. The air then travels axially from the back of the chamber to the front. The air exits the inner chamber radially through the diffuser holes at the front of the chamber into the annular cavity between the chamber and door. The air exits the annular cavity through a port in the bottom of the chamber door. The design of the test chamber encourages laminar flow of the air through its interior. With the maximum flow rate possible with the generator, 150 L/min, the air in the ~40 L chamber is displaced approximately once every 16 s. With the axial chamber length of 41 cm, the velocity of the passing air corresponding to this displacement is 2.6 cm/s. The Reynolds number (Re) of this flow for a kinematic viscosity of $1.6 \times 10^{-5} \text{ m}^2/\text{s}$ (air at 20 °C) in a circular container of diameter 35 cm is then $Re \cong 560$, well below the laminar-turbulent threshold of 2300.

Commercial platinum resistance thermometers (PRTs) are mounted inside the test chamber and inside the environmental chamber (but outside the test chamber) for the purpose of monitoring the temperature in those locations. The test chamber PRT is cylindrical in shape and has a diameter of 0.25 cm and a length of 1.5 cm. It is placed in the center of the chamber by attaching it using cable ties to a 0.16 cm vertical rod that is placed at approximately the axial midpoint of the chamber, as shown in Fig. 14. The test chamber PRT has been calibrated by the NIST Thermodynamic Metrology Group and serves as the reference thermometer for determining the chamber temperature during calibrations. The temperature inside the environmental chamber is specified to be stable and uniform to within 0.5 °C. The thermal mass of the test chamber walls further stabilizes the temperature inside of the chamber. It will be shown in section 6.3 that inside the central part of the test chamber the temperature is stable and uniform to within ± 10 mK. When calibrating customer thermohygrometers, they are placed as close as possible to the reference thermometer without blocking them from the air flow.

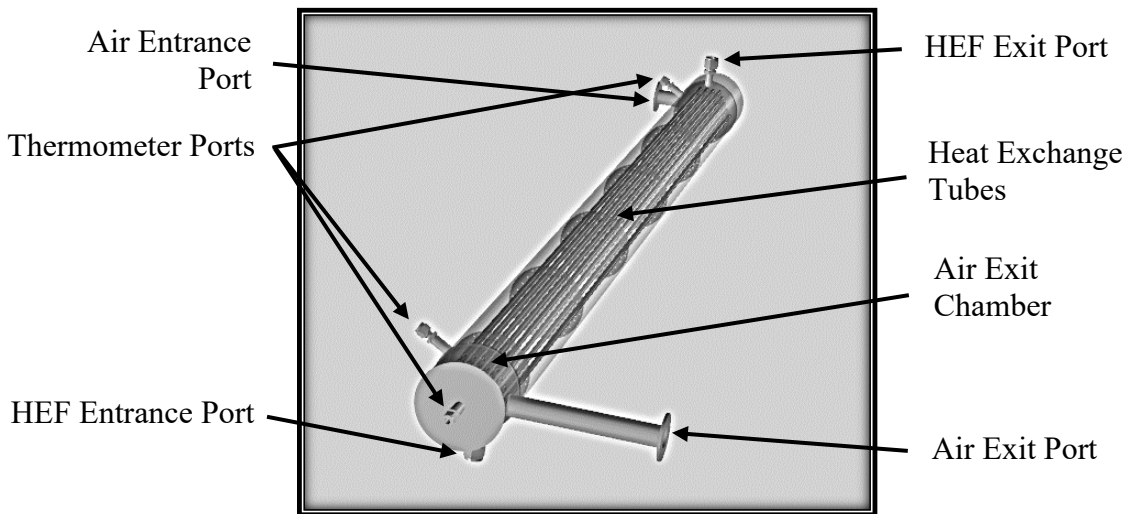
6.2. Heat Exchanger Design

The humidified air exiting the HHG is conditioned to the temperature of the test chamber before it enters the chamber. The conditioning is performed using a counterflow heat exchanger. Semi-transparent diagrams of this heat exchanger are shown in Fig. 15. The heat exchanger is made of 316L stainless steel and uses a commercial heat-exchange fluid (labeled HEF in figure). The heat-exchange fluid is circulated into the exchanger from a commercial dynamic temperature-control system. The outside of the exchanger consists of an outer-shell tube of diameter 10 cm and length 153 cm that is bounded on each end by a circular plate. Immediately inside each of the two tube ends is a cylindrical chamber of diameter 10 cm and length 6 cm; one is an air-entrance chamber and the other is an air exit chamber. Between these two chambers are 48 open heat-exchange thin-wall tubes of diameter 0.63 cm, length 140 cm, and wall thickness 0.09 cm. The heat-exchange tubes are all parallel to the outer-shell tube and are mounted in holes in the inside walls of the chambers. The tubes are evenly spaced in a hexagonal lattice using 6 circular mounting plates (shown in Fig. 16) spaced at 28 cm intervals. Each mounting plate contains small holes of diameter 0.2 cm to allow the heat-exchange fluid to flow through. The fluid flows into the large tube through a port located just inside the air exit chamber and exits through a port located just inside the air entrance chamber. The air enters the heat exchanger through an entrance port attached to the air entrance chamber, passes through the heat-exchange tubes into the air exit chamber, and exits through an exit port. PRTs are mounted in ports attached to the ends of the outer-shell tube for the

purpose of monitoring the temperature in the air-entrance and air-exit chambers. Two other PRTs are mounted in ports adjacent to the heat-exchange-fluid-entrance and heat-exchange-fluid-exit ports for the purpose of monitoring the temperature in those locations. The counterflow design ensures that the temperature of the air exiting the heat exchanger is approximately equal to the temperature of the heat-exchange fluid entering the heat exchanger. By controlling the heat-exchange fluid temperature to be that of the test chamber, the temperature non-uniformities in the test chamber can be kept to within 0.01 °C even when flowing humidified air through it at 150 L/min.



(a) Side View



(b) Front View

Figure 15. Diagrams of the heat exchanger, showing a) side view and b) front view

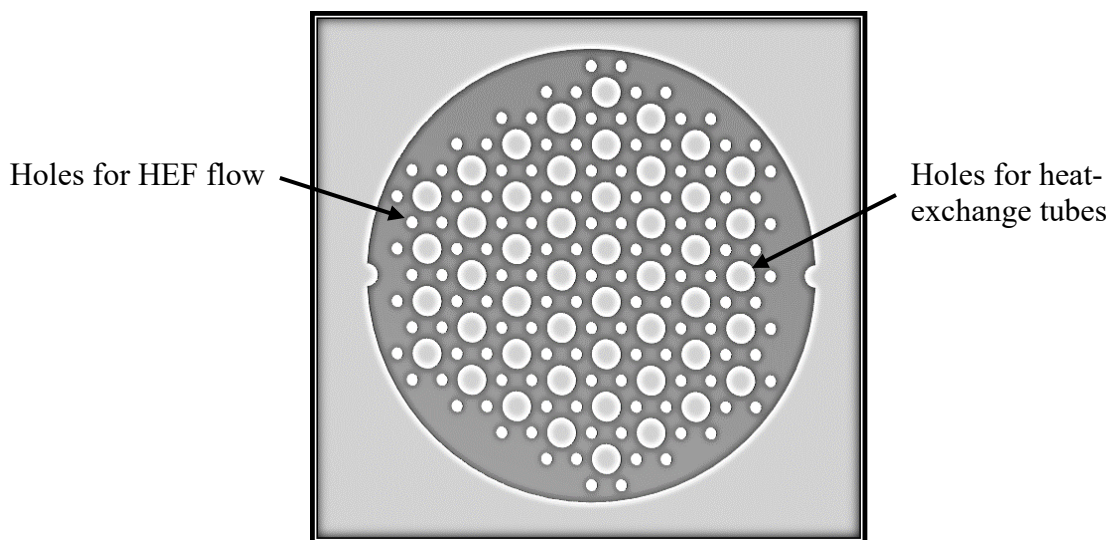


Figure 16. Diagram of a mounting plate in the heat exchanger

Both the environmental chamber and heat exchanger can be controlled at temperatures between $-34\text{ }^{\circ}\text{C}$ and $190\text{ }^{\circ}\text{C}$. This allows calibration of thermohygrometers over the relative humidity range 2 % to 98 % for temperatures between $-34\text{ }^{\circ}\text{C}$ and $85\text{ }^{\circ}\text{C}$, as well as over more limited relative-humidity ranges between $85\text{ }^{\circ}\text{C}$ and $190\text{ }^{\circ}\text{C}$.

6.3. Validation Tests

The test chamber was examined for both temperature stability and non-uniformity. Figure 17 shows plots of the temperature as a function of time inside the test chamber once a steady-state temperature has been achieved (typically after several hours). These plots reveal the temperature stability inside the chamber over a period of 7000 s at temperatures of approximately $-40\text{ }^{\circ}\text{C}$, $20\text{ }^{\circ}\text{C}$, and $80\text{ }^{\circ}\text{C}$, when 150 L/min of air flows through the chamber. The peak-to-peak variation of the temperature is approximately 5 mK. Figure 18 shows the temperature uniformity inside the test chamber when 150 L/min of air flows through the chamber, through measurements of the temperature difference between the two junctions of a differential thermocouple. The junctions were attached to the rod shown in Fig. 14 and placed 15 cm from the center of the rod, separating them from each other by 30 cm. The rod was placed in four different positions in the chamber. In all positions, the center of the rod was approximately in the center of the test chamber. In one case, the rod was placed vertically (as in Fig. 14). In a second case, it was placed horizontally, perpendicular to the chamber axis. In a third case, the rod was placed along the axis of the chamber. In the final case, radial temperature variations were measured by placing one of the thermocouple junctions in the center of the rod and the other junction 15 cm away; the rod was placed vertically and azimuthal symmetry was assumed for this arrangement. The temperature-difference measurements were made at five different temperatures: $-40\text{ }^{\circ}\text{C}$, $0\text{ }^{\circ}\text{C}$, $20\text{ }^{\circ}\text{C}$, $50\text{ }^{\circ}\text{C}$, and $80\text{ }^{\circ}\text{C}$. The vertical, horizontal, and radial temperature differences were all within 12 mK. The axial temperature differences were the largest, increasing from 2 mK at $80\text{ }^{\circ}\text{C}$ to 30 mK at $-40\text{ }^{\circ}\text{C}$. Based on the results of Figs. 17-18, and considering the close placement of customer thermohygrometers to the reference thermometer, we estimate the chamber temperature standard uncertainty due to stability and uniformity to be 10 mK.

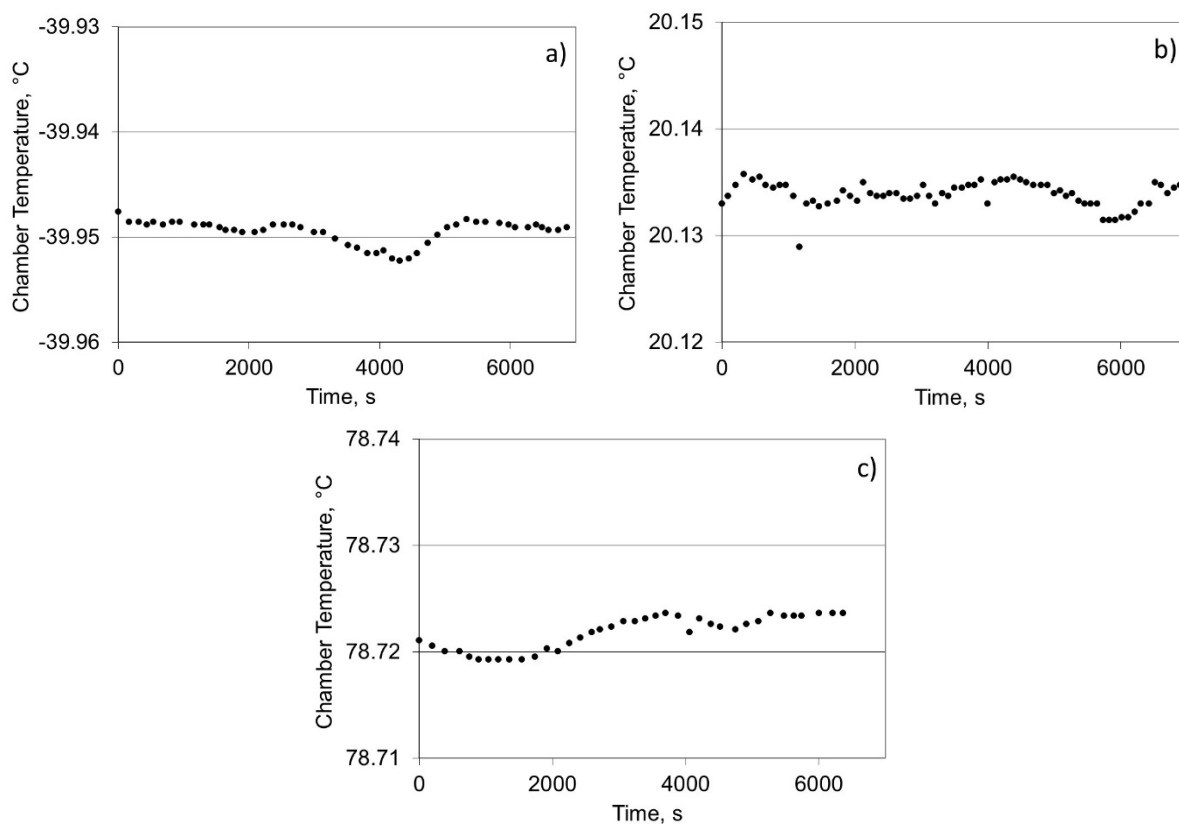


Figure 17. Temperature stability in test chamber near a) $-40\text{ }^{\circ}\text{C}$, b) $20\text{ }^{\circ}\text{C}$, and c) $80\text{ }^{\circ}\text{C}$

Figure 19 shows the stability of the relative humidity inside the test chamber at $23\text{ }^{\circ}\text{C}$ at three different values of generated relative humidity: 80 %, 20 %, and 5 %, with a flow rate of 150 L/min. The standard deviation of the RH values is 0.014 %, 0.022 %, and 0.002 % for the RH values of 80 %, 20 %, and 5 %, respectively.

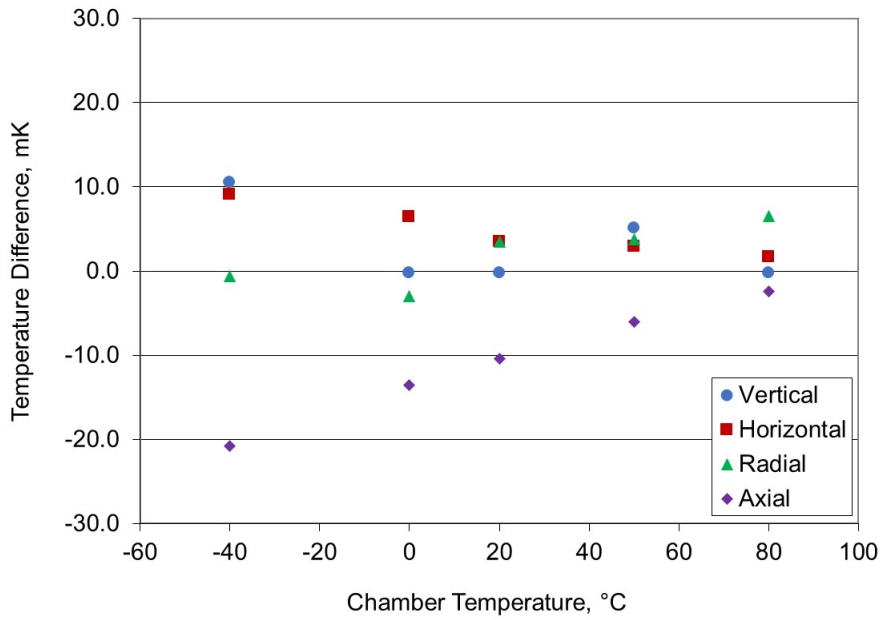


Figure 18. Temperature difference between two locations in test chamber (see text for location description) separated by 30 cm, measured using differential thermocouples

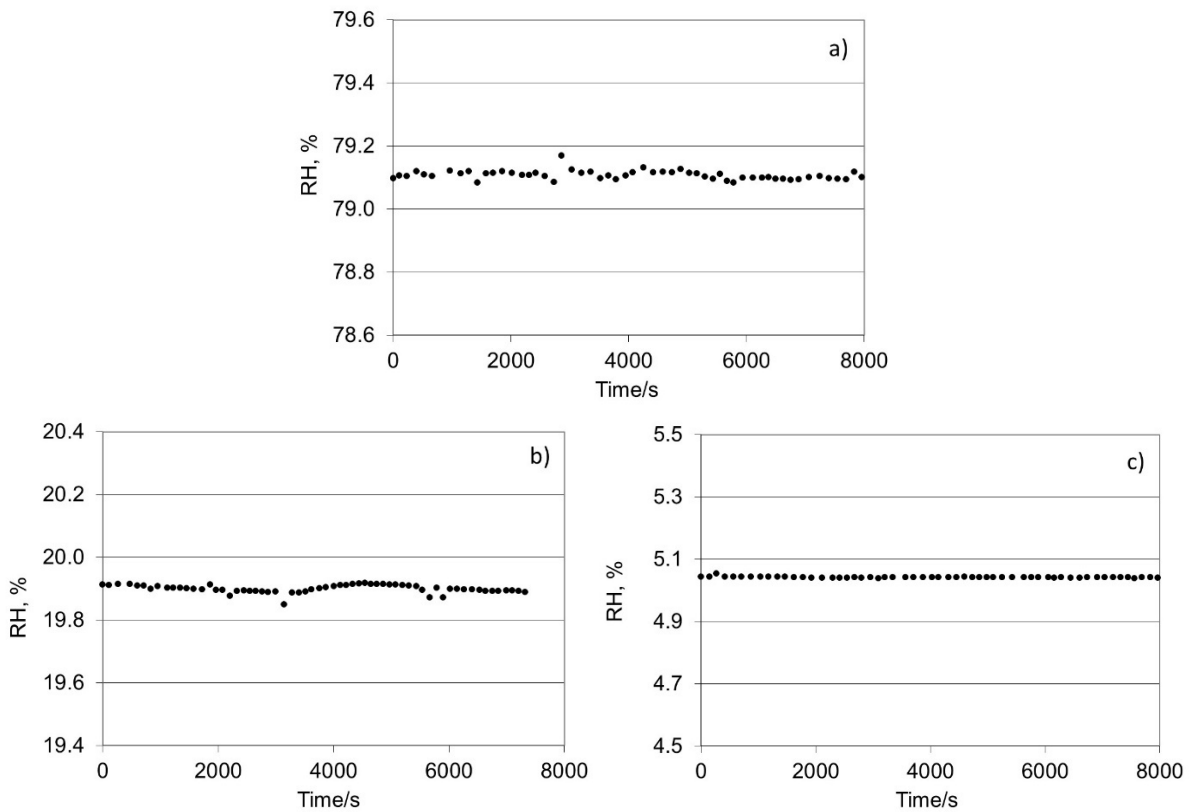


Figure 19. Stability of relative humidity in test chamber

7. Uncertainty Budget

Based on these performance tests as well as measurement equipment specifications, we have constructed uncertainty budgets for the humidity generated by the HHG. There are budgets for the three expressions of humidity (water amount fraction, dew/frost-point temperature, and relative humidity) under two conditions: two-pressure generator without dilution and two pressure with dilution. The total uncertainties associated with these budgets are based on the guidelines for the expression of uncertainty in measurement [13,14]. The equations relating the total uncertainties to the uncertainty components are listed below and derived in Appendix I.

The total uncertainty for humidity generated by the hybrid generator is presented here for four different humidity definitions: water amount fraction, dew/frost-point temperature, relative humidity, and water mass ratio. For each of these four definitions, we present the uncertainty for the cases of humidity generated in 1-P mode, 2-P mode, and divided-flow mode. In the equations below, $u(X)$ is the standard uncertainty of the quantity X .

7.1. Uncertainty Equations

7.1.1. Water Amount Fraction Generated in 1-P or 2-P Mode

Here, the total standard relative uncertainty for the water amount fraction, $u_r(x)$, is expressed as

$$u_r(x)^2 = \left[\frac{u(x)}{x} \right]^2 = \left(\frac{1}{e_s} \frac{de_s}{dT_s} \right)^2 u(T_s)^2 + \frac{u(P_s)^2}{P_s^2} + \frac{u(e_s^{\text{calc}})^2}{e_s^2} + \frac{u(f_s^{\text{calc}})^2}{f_s^2}. \quad (7)$$

The four relevant uncertainties are $u(T_s)$, $u(P_s)$, $u(e_s^{\text{calc}})$, and $u(f_s^{\text{calc}})$. Here, $u(e_s^{\text{calc}})$ and $u(f_s^{\text{calc}})$ are the uncertainties of the calculated values of $e(T_s)$ and $f_s(T_s, P_s)$, respectively, due to the imperfect knowledge of these physical relations.

7.1.2. Dew-point Temperature Generated in 1-P or 2-P Mode

For this case, the total standard uncertainty of the dew-point temperature T_{DP} or frost-point temperature T_{FP} of the gas in a test chamber with pressure P_c and temperature $T_c = T_{\text{DP}}$ or $T_c = T_{\text{FP}}$ is expressed as

$$u(T_{\text{DP}})^2 = \left(\frac{e_c}{[de_c/dT_{\text{DP}}]} \right)^2 \left[\left(\frac{1}{e_s} \frac{de_s}{dT_s} \right)^2 u(T_s)^2 + \frac{u(P_s)^2}{P_s^2} + \frac{u(P_c)^2}{P_c^2} + u_r(\Delta e^{\text{calc}})^2 + u_r(\Delta f^{\text{calc}})^2 \right] \quad (8)$$

The five relevant uncertainties are $u(T_s)$, $u(P_s)$, $u(P_c)$, $u_r(\Delta e^{\text{calc}})$, and $u_r(\Delta f^{\text{calc}})$. When the generator is used in 1-P mode ($P_s \cong P_c$),

$$u_r(\Delta e^{\text{calc}}) = u_r(\Delta f^{\text{calc}}) = 0. \quad (9)$$

When the generator is used in 2-P mode ($P_s \neq P_c$),

$$u_r(\Delta e^{\text{calc}})^2 \equiv \frac{u(e_s^{\text{calc}})^2}{e_s^2} + \frac{u(e_c^{\text{calc}})^2}{e_c^2}, \quad (10)$$

$$u_r(\Delta f^{\text{calc}})^2 \equiv \frac{u(f_s^{\text{calc}})^2}{f_s^2} + \frac{u(f_c^{\text{calc}})^2}{f_c^2}. \quad (11)$$

Here, $u(e_s^{\text{calc}})$, $u(e_c^{\text{calc}})$, $u(f_s^{\text{calc}})$, and $u(f_c^{\text{calc}})$ are the uncertainties of the calculated values of, $e(T_s)$, $e(T_c)$, $f(T_s, P_s)$, and $f(T_c, P_c)$, respectively, due to the imperfect knowledge of these physical relations. In Eqs. 10-11, note that the subscript “r” in $u_r(\Delta e^{\text{calc}})$ and $u_r(\Delta f^{\text{calc}})$ is used to show that they are relative uncertainties and therefore dimensionless.

7.1.3. Relative Humidity Generated in 1-P or 2-P Mode

The total standard relative uncertainty for the relative humidity, $u_r(RH)$, of the gas in the test chamber with temperature T_c and pressure P_c is expressed as

$$u_r(RH)^2 = \left[\frac{u(RH)}{RH} \right]^2 = \left[\left(\frac{1}{e_s} \frac{de_s}{dT_s} \right)^2 u(T_s)^2 + \frac{1}{P_s^2} u(P_s)^2 + \left(\frac{1}{e_c} \frac{de_c}{dT_c} \right)^2 u(T_c)^2 + \frac{1}{P_c^2} u(P_c)^2 + u_r(\Delta e^{\text{calc}}) + u_r(\Delta f^{\text{calc}}) \right]^2 \quad (12)$$

The six relevant uncertainties are $u(T_s)$, $u(P_s)$, $u(T_c)$, $u(P_c)$, $u_r(\Delta e^{\text{calc}})$, and $u_r(\Delta f^{\text{calc}})$. Here, $u_r(\Delta e^{\text{calc}})$ and $u_r(\Delta f^{\text{calc}})$ are given by Eqs. 9 for 1-P mode and Eqs. 10–11 for 2-P mode.

7.1.4. Water Amount Fraction Generated in Divided-flow Mode

For this case, the total standard relative uncertainty for the water amount fraction, $u_r(x)$ is expressed as

$$u_r(x)^2 = \left[\frac{u(x)}{x} \right]^2 \equiv \left(\frac{1}{e_s} \frac{de_s}{dT_s} \right)^2 u(T_s)^2 + \frac{u(P_s)^2}{P_s^2} + \frac{u(e_s^{\text{calc}})^2}{e_s^2} + \frac{u(f_s^{\text{calc}})^2}{f_s^2} + \frac{u(\dot{n}_p)^2}{\dot{N}^2} + \left(\frac{x_s}{x} - 1 \right)^2 \left(\frac{u(x_p)^2}{x_s^2} + \frac{u(\dot{n}_s)^2}{\dot{N}^2} \right) \quad (13)$$

The seven relevant uncertainties are $u(T_s)$, $u(P_s)$, $u(e_s^{\text{calc}})$, $u(f_s^{\text{calc}})$, $u(x_p)$, $u(\dot{n}_s)$, and $u(\dot{n}_p)$.

7.1.5. Frost-point Temperature Generated in Divided-flow Mode

In the hybrid generator, the divided flow method will only be used for generating frost points. Here, the total standard uncertainty of the frost-point temperature T_{DP} of the gas in the test chamber is

$$u(T_{FP})^2 = \frac{e_c}{[de_c/dT_c]^2} \left[\left(\frac{1}{e_s} \frac{de_s}{dT_s} \right)^2 u(T_s)^2 + \frac{u(P_s)^2}{P_s^2} + \frac{u(P_c)^2}{P_c^2} + u_r(\Delta e^{\text{calc}})^2 + u_r(\Delta f^{\text{calc}})^2 \right. \\ \left. + \left(\frac{x_s}{x} - 1 \right)^2 \left(\frac{u(x_p)^2}{x_s^2} + \frac{u(\dot{n}_s)^2}{\dot{N}^2} \right) + \frac{u(\dot{n}_p)^2}{\dot{N}^2} \right] \quad (14)$$

The eight relevant uncertainty elements are $u(T_s)$, $u(P_s)$, $u(x_p)$, $u(\dot{n}_s)$, $u(\dot{n}_p)$, $u(P_c)$, $u_r(\Delta e^{\text{calc}})$, and $u_r(\Delta f^{\text{calc}})$. Here, $u_r(\Delta e^{\text{calc}})$ and $u_r(\Delta f^{\text{calc}})$ are defined in Eqs. 10-11.

7.1.6. Relative Humidity Generated in Divided-flow Mode

Here, the total standard relative uncertainty of the relative humidity of the gas in the test chamber is

$$u_r(RH) = \left[\frac{u(RH)}{RH} \right]^2 = \left[\left(\frac{1}{e_s} \frac{de_s}{dT_s} \right)^2 u(T_s)^2 + \frac{u(P_s)^2}{P_s^2} + \left(\frac{1}{e_c} \frac{de_c}{dT_c} \right)^2 u(T_c)^2 + \frac{u(P_c)^2}{P_c^2} \right. \\ \left. + u_r(\Delta e^{\text{calc}}) + u_r(\Delta f^{\text{calc}}) + \left(\frac{x_s}{x} - 1 \right)^2 \left(\frac{u(x_p)^2}{x_s^2} + \frac{u(\dot{n}_s)^2}{\dot{N}^2} \right) + \frac{u(\dot{n}_p)^2}{\dot{N}^2} \right] \quad (15)$$

The nine relevant uncertainty elements are $u(T_s)$, $u(P_s)$, $u(T_c)$, $u(P_c)$, $u_r(\Delta e^{\text{calc}})$, $u_r(\Delta f^{\text{calc}})$, $u(x_p)$, $u(\dot{n}_s)$, and $u(\dot{n}_p)$, where $u_r(\Delta e^{\text{calc}})$ and $u_r(\Delta f^{\text{calc}})$ are given by Eqs. 10-11.

7.1.7. Water Mass Ratio

The total standard uncertainty for mass ratio is related to that for the amount fraction by

$$u(r) = 0.62196 \frac{1}{(1-x)^2} u(x), \quad (16)$$

or, in terms of relative uncertainty $u_r(r)$,

$$u_r(r) = \frac{u(r)}{r} = \frac{1}{(1-x)} u_r(x) \quad (17)$$

Here, $u_r(x)$ is given by Eq. 7 when the generator is used in 1-P or 2-P mode, and by Eq. 13 when the generator is used in divided-flow mode.

7.2. Uncertainty Elements

Shown in Table 1 is a list of all the relevant uncertainty elements mentioned above and their standard uncertainty values. The subcomponents of the uncertainty elements T_s , P_s , and P_c are given in Appendix II. For calibration of a chilled-mirror hygrometer with an external thermometer, the value for the uncertainty of T_c is based on the typical uncertainty for the calibration of external temperature probes at NIST [15]. For calibration of relative humidity sensors in the HHG test chamber, the uncertainty of T_c additionally contains a component for temperature differences between the sensor and the chamber standard thermometer. In Table 1, the uncertainty for the calculation of $e(T)$ is obtained from Fig. 6.4 of [16] for $T \geq 0.01$ °C and from Eq. 5a of [9] for $T < 0.01$ °C (note that Eq. 5a provides an expanded uncertainty that must be divided by 2). The uncertainties for the calculations of f_s and f_c are presented as a fit to the uncertainty data of Table 9 in [17]; because there is no data below -50 °C, we extrapolated the curve determined from the available data to obtain the uncertainty formula listed in Table 1. In obtaining the formula, the “maximum percentage uncertainties” from [17] were divided by $\sqrt{3}$ to obtain the standard uncertainty. The values for $u(f_s^{\text{calc}})$ and $u(f_c^{\text{calc}})$ decrease with temperature and increase with pressure; they are quite significant for some operating conditions. By comparison, the uncertainties of e_s^{calc} and e_c^{calc} are negligible.

An additional uncertainty element is that due to moisture diffusion through the vertical pressure sensing tube of the final saturator. When the saturator temperature is above ambient, moisture will condense inside the tube in the ambient-temperature region and drip down to the saturator. As the air in that region dries from the condensation, additional moisture will diffuse through the tube from the saturator to the ambient-temperature region. This creates a diffusion-driven moisture flow which can lower the water amount fraction of the air exiting the saturator. We have calculated the depletion and determined it to be less than 0.002 % for the intended gas flows through the generator (over 20 L/min). This amount is negligible compared to other uncertainties, and as a result we are not including it in Table 1.

The table does not include uncertainties from measurement repeatability of the particular hygrometer under calibration. In the calibration reports, however, the total uncertainty for the calibration of the hygrometer is reported, with the uncertainty due to hygrometer repeatability determined as described in the hygrometer specifications. If repeatability is not provided in the manufacturer specifications, the repeatability of similar instruments is used.

Table 1. Uncertainty elements for the Hybrid Humidity Generator and their uncertainties. Here, $u(X)$ is the standard uncertainty for element X . The elements with subscript “c” refer to the environment in which the humidity is to be determined. The element T_c is only relevant for chilled-mirror hygrometers with an external thermometer for determination of relative humidity or for thermohygrometers calibrated inside the test chamber. Note that the values for T_s in the expressions for $u(f_s^{\text{calc}})$ and $u(f_c^{\text{calc}})$ are in units of Kelvin.

X	$u(X)$ ($k = 1$)	Condition	Unit
T_s	1.5 $0.16T_s/^\circ\text{C} - 4.9$	$(T \leq 40^\circ\text{C})$ $(T > 40^\circ\text{C})$	mK
P_s	18 $\sqrt{29^2 + (P_s / 10000 \text{ Pa})^2}$	$(P_s \approx \text{ambient pressure})$ $(P_s > \text{ambient pressure})$	Pa
T_c	10 15	CM external thermometer Use of test chamber	mK
P_c	15		Pa
e_s^{calc}	See Fig. 6.4 of [16]		Pa
f_s^{calc}	$P_s / (10^7 \cdot \text{Pa}) (18.3 \text{ K} / T_s - 0.047)$		--
e_c^{calc}	From Fig. 6.4 of [16] From Eq. 5a of [9]	$T \geq 0.01^\circ\text{C}$ $T < 0.01^\circ\text{C}$	Pa
f_c^{calc}	$P_c / (10^7 \cdot \text{Pa}) (18.3 \text{ K} / T_c - 0.047)$		--
x_p	1		$\text{nmol} \cdot \text{mol}^{-1}$
\dot{n}_s	$5 \times 10^{-4} \dot{n}_s$ $1 \times 10^{-3} \dot{n}_s$	$(\dot{n}_s \geq 7.5 \times 10^{-6} \text{ mol} \cdot \text{s}^{-1})$ $(\dot{n}_s < 7.5 \times 10^{-6} \text{ mol} \cdot \text{s}^{-1})$	$\text{mol} \cdot \text{s}^{-1}$ $\text{mol} \cdot \text{s}^{-1}$
\dot{n}_p	$5 \times 10^{-4} \dot{n}_p$		$\text{mol} \cdot \text{s}^{-1}$

7.3. Uncertainty Plots

Figure 20 shows the total expanded uncertainty for humidity generated by the HHG when the generator is operated in 1-P mode. The uncertainty is shown for the a) water amount fraction (relative uncertainty) and b) dew point. Here, the total expanded uncertainty is given by $U(x) = ku(x)$, where the coverage factor is $k = 2$. The expanded relative uncertainty is given by $U_r(x) = U(x)/x$. In the figure, the black curve represents the total uncertainty, while the other curves represent the contributions to the total uncertainty from individual uncertainty components. In Fig. 20(b), the uncertainty contributions from e_s^{calc} and e_c^{calc} are zero, because these uncertainties cancel out when the generator is used in 1-P mode; the uncertainty contributions for f_s^{calc} and f_c^{calc}

are zero for the same reason. Also in this plot, the curve designated as “*P*” represents the contributions from both P_s and P_c . The figure shows that for the 1-P mode, the dominant uncertainty is from pressure measurement and stability, except for saturator temperatures above 60 °C; in this case uncertainties due to temperature non-uniformities in the bath dominate. Figures 21(a) and 21(b) show similar plots for the case when the generator is operated in 2-P mode with $P_s = 500$ kPa. In Fig. 21(b), the discontinuity at 0 °C is due to the assumption of frost-point generation below this temperature. This figure shows that when the saturator is operated in this way, the uncertainties in f_s^{calc} and f_c^{calc} usually dominate.

Figure 22 shows the expanded uncertainty generated by the HHG when it is used in divided-flow mode. The uncertainties plotted are (a) the water amount fraction (relative uncertainty) and (b) the frost-point temperature. For these plots, the saturator parameters are $P_s = 300$ kPa and $T_s = 0.5$ °C. In the plots, “*n*” refers to the combined contribution to the total from \dot{n}_s and \dot{n}_p . In Fig 22(a), $U_r(x)$ is relatively constant for $x > 2 \times 10^{-6}$. At the highest value of x shown in the plot, $\dot{n}_p = 0$ and so $U_r(x)$ is only due to the saturator. As x decreases to 2×10^{-6} , $U_r(x)$ increases slightly due to the rising significance of $u(\dot{n}_s)$ and $u(\dot{n}_p)$. As x decreases below 2×10^{-6} , $u(x_p)/x$ dominates $U_r(x)$, increasing its value to nearly 2 % at $x = 1 \times 10^{-7}$. In (b), the total expanded uncertainty is $U(T_{\text{FP}}) = ku(T_{\text{FP}})$. For -70 °C $\leq T_{\text{FP}} \leq -12$ °C, $U(T_{\text{FP}})$ ranges from 16 mK to 25 mK, decreasing with temperature. As T_{FP} decreases below -70 °C, $U(T_{\text{FP}})$ rises rapidly up to 120 mK at -90 °C due to the increasing influence of $u(x_p)$.

Figure 23 shows the expanded relative uncertainty $U_r(RH) = U(RH)/RH$ for relative humidity calibrations of a chilled-mirror hygrometer with an external temperature probe, using humid gas generated by the HHG and flowing to an environment with temperature $T_c = 20$ °C and pressure 100 kPa. Here, $U_r(RH)$ includes the uncertainty of the humidity produced by the generator and the uncertainty of the calibration of the hygrometer’s external temperature probe. In plots a) and b), the generator is operated in 2-P mode; the plots show the uncertainty for two saturator temperatures: a) $T_s = 20$ °C and b) $T_s = 1$ °C, which generate different relative humidity ranges. In plot c), the generator is operated in divided-flow mode.

Figure 24 shows the expanded relative uncertainty $U_r(RH) = U(RH)/RH$ for relative humidity calibrations of a thermohygrometer, using humid gas generated by the HHG and flowing to the test chamber with temperature $T_c = 20$ °C and pressure 100 kPa. Here, $U_r(RH)$ includes the uncertainty of the humidity produced by the generator and the uncertainty of the temperature in the chamber at the point of the thermohygrometer. In plots a) and b), the generator is operated in 2-P mode; the plots show the uncertainty for two saturator temperatures: a) $T_s = 20$ °C and b) $T_s = 1$ °C, which generate different relative humidity ranges. In plot c), the generator is operated in divided-flow mode. The primary difference between the plots in Figs. 23 and 24 is that for Fig. 23 $u(T_c) = 0.01$ °C and for Fig. 24 $u(T_c) = 0.015$ °C.

Figure 25 shows the total expanded relative uncertainty for mass ratio, $U_r(r) = U(r)/r$, generated by the HHG when the generator is operated in a) 1-P mode and b) 2-P mode with $P_s = 500$ kPa. In the plots, the black curve represents the total uncertainty, while the other curves represent the contributions to the total uncertainty from individual uncertainty components.

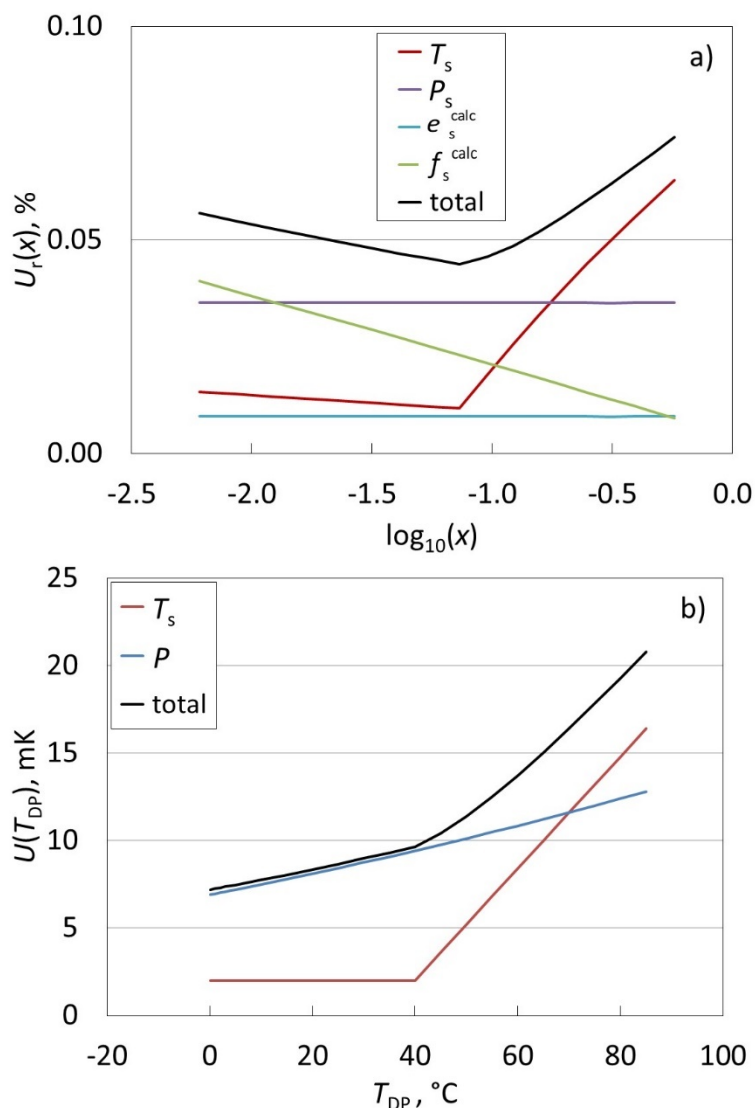


Figure 20. Total expanded uncertainty U for the (a) water amount fraction and (b) dew-point temperature generated by the HHG saturator when used in 1-P mode. The black curve represents the total uncertainty, while the other curves show the contributions from individual uncertainty elements. In a), the expanded uncertainty is expressed as a relative uncertainty $U_r(x) = U(x)/x = ku(x)/x$, where $k = 2$ and $u(x)$ is the standard uncertainty for x . In b), the total expanded uncertainty is $U(T_{\text{DP}}) = ku(T_{\text{DP}})$. In b), P represents the combined contributions from both P_s and P_c .

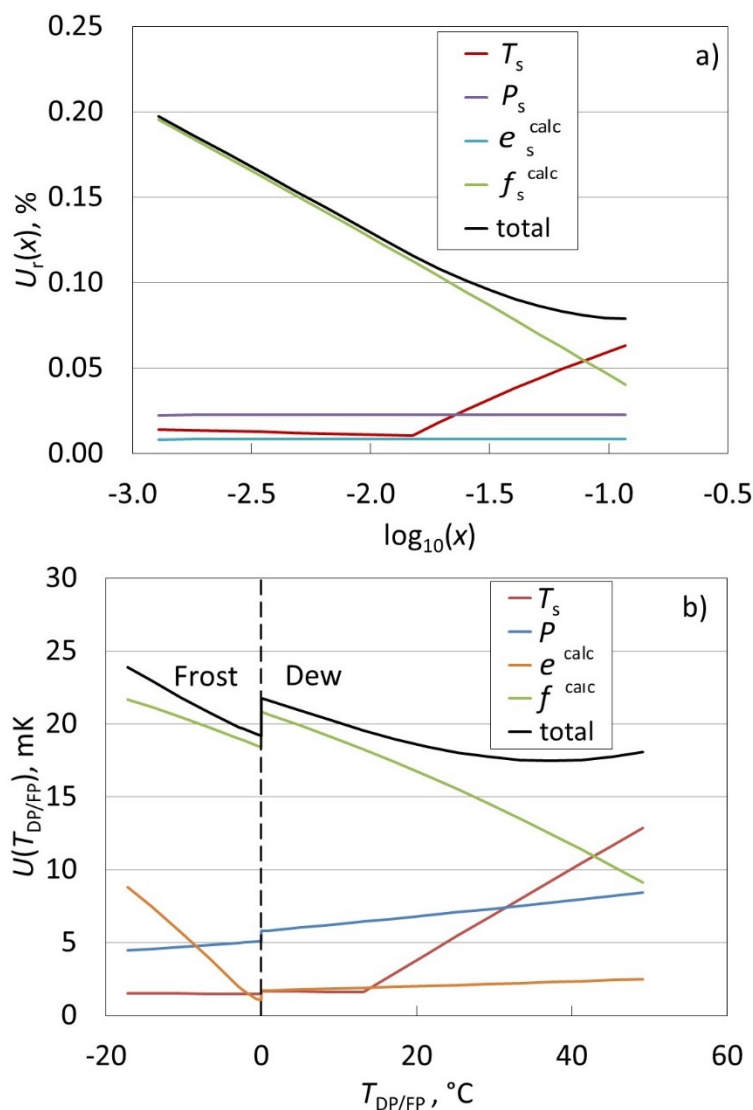


Figure 21. Total expanded uncertainty U for the (a) water amount fraction and (b) dew/frost-point temperature generated by the HHG saturator when used in 2-P mode with $P_s = 500$ kPa. The black curve represents the total uncertainty, while the other curves show the contributions from individual uncertainty elements. In a), the expanded uncertainty is expressed as a relative uncertainty $U_r(x) = U(x)/x = ku(x)/x$, where $k = 2$ and $u(x)$ is the standard uncertainty for x . In b), the total expanded uncertainty is $U(T_{\text{DP}}) = ku(T_{\text{DP}})$. In b), P , e^{calc} , and f^{calc} each represent the combined contributions of their quantity from both the saturator and chamber (hygrometer).

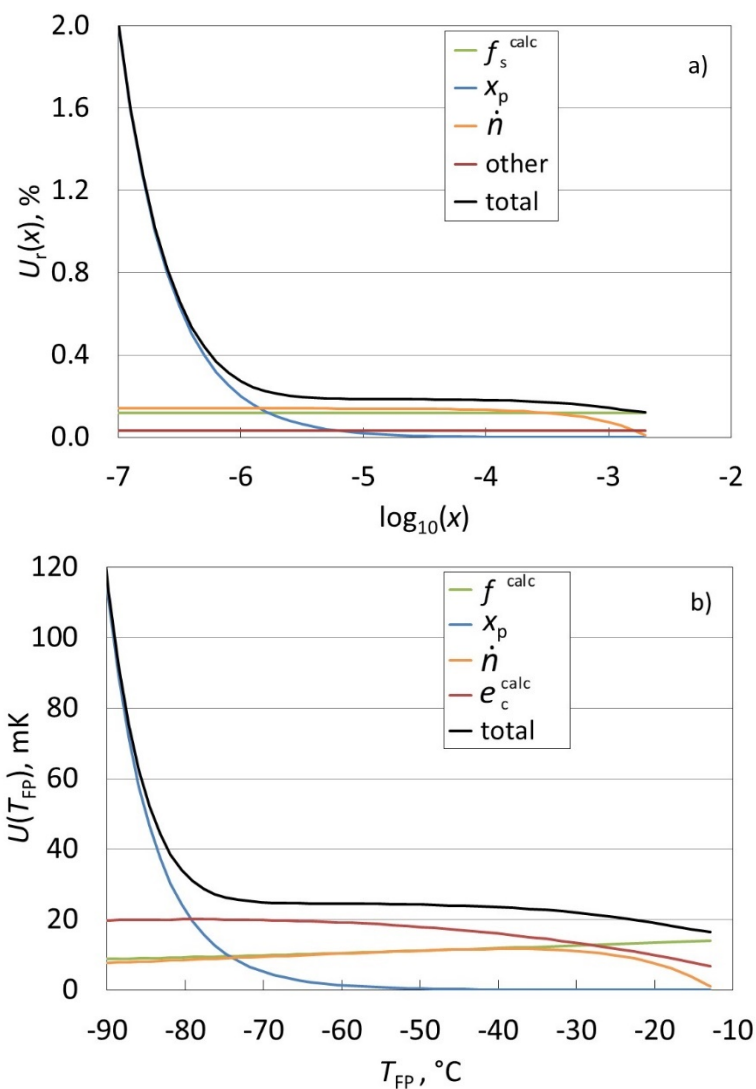


Figure 22. Total expanded uncertainty for the a) water amount fraction (relative uncertainty) and b) frost-point temperature generated by the HHG when it is used in divided-flow mode with a saturator pressure of $P_s = 300$ kPa. Here, f^{calc} represents the combined uncertainty contributions from both the saturator and chamber (hygrometer), and \dot{n} represents the combined uncertainty contributions from the wet gas and dry gas.

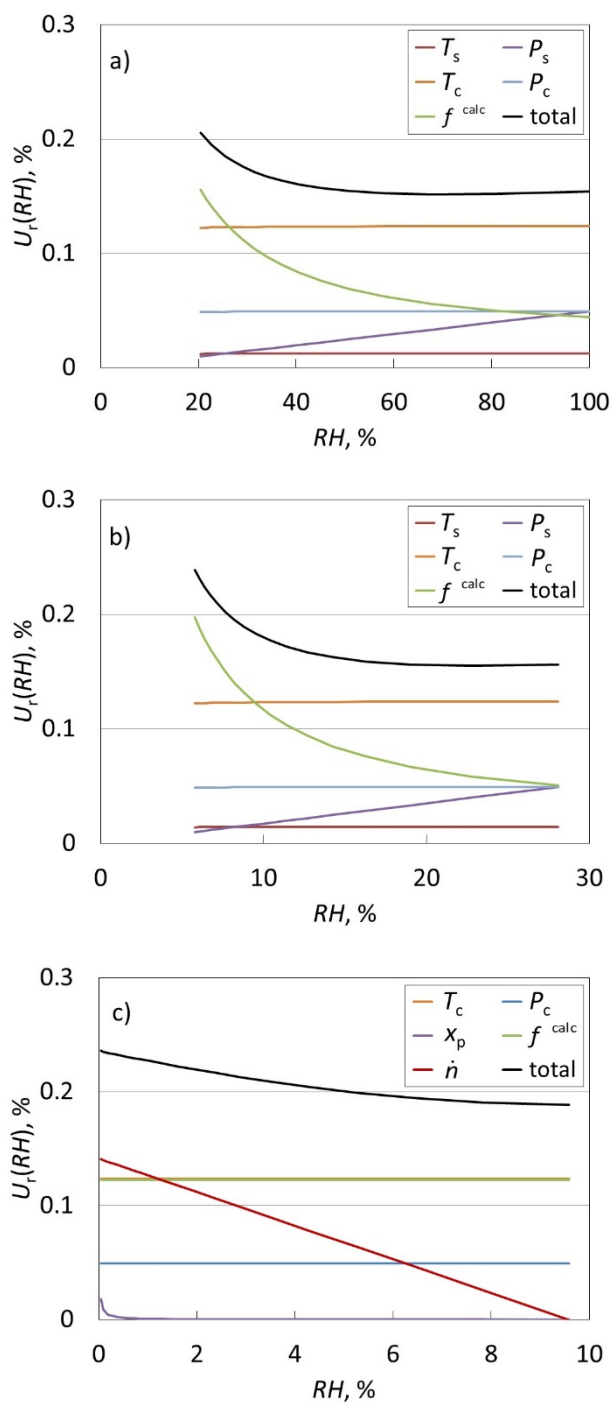


Figure 23. Total expanded relative uncertainty $U_r(RH)$ for the relative humidity calibrations of a chilled-mirror hygrometer with and external temperature probe, using humid gas generated by the HHG to an environment of temperature $T_c = 20$ °C and pressure $P_c = 100$ kPa. Here, $U_r(RH)$ includes the uncertainty for the calibration of the hygrometer's external temperature probe. In plots a) and b), the generator is used in 2-P mode, and the saturator temperature is a) 20 °C and b) 1 °C; the relative humidity is varied by changing the saturator pressure. In c), the generator is used in divided-flow mode.

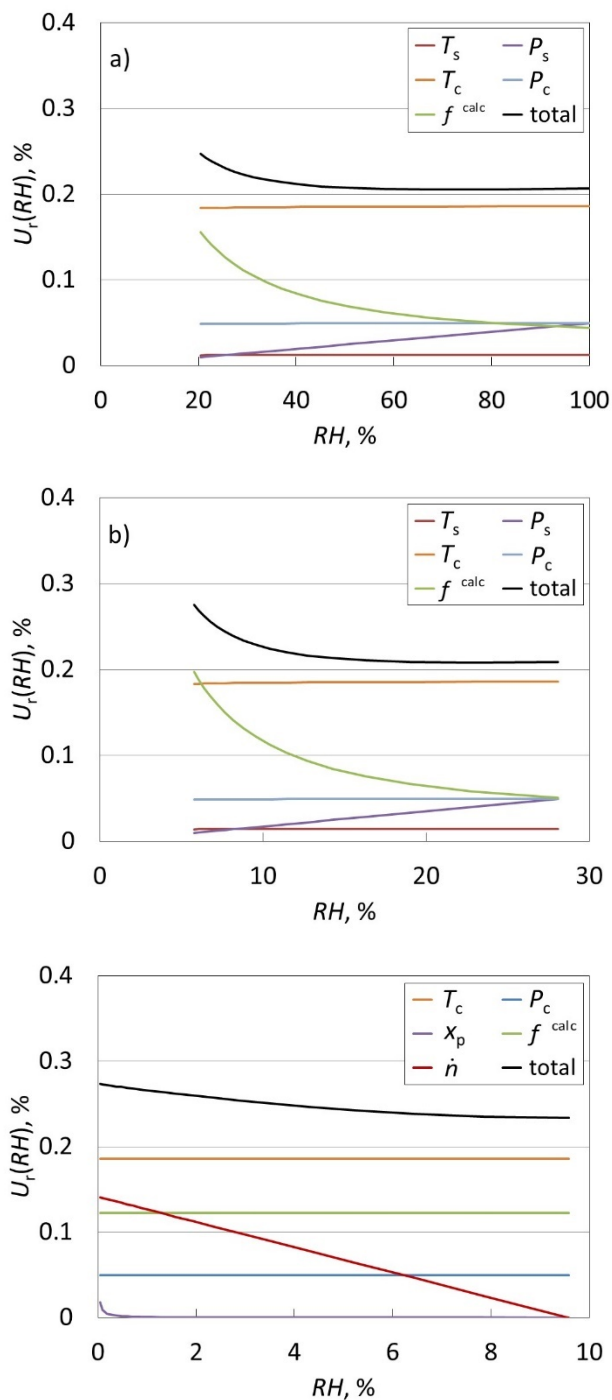


Figure 24. Total expanded relative uncertainty $U_r(RH)$ for the relative humidity calibrations of a thermohygrometer, using humid gas generated by the HHG to the test chamber with temperature $T_c = 20$ °C and pressure $P_c = 100$ kPa. Here, $U_r(RH)$ includes the uncertainty for the temperature of the chamber at the location of the thermohygrometer. In plots a) and b), the generator is used in 2-P mode, and the saturator temperature is a) 20 °C and b) 1 °C; the relative humidity is varied by changing the saturator pressure. In c), the generator is used in divided-flow mode.

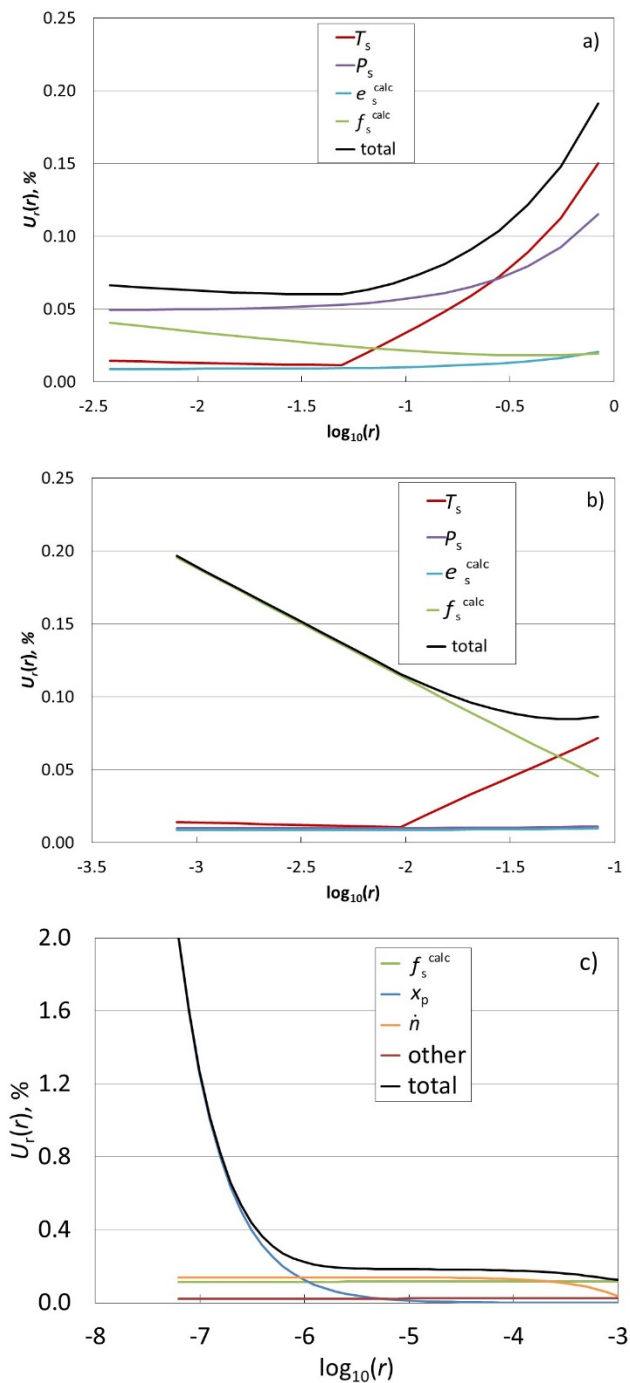


Figure 25. Total expanded relative uncertainty $U_T(r)$ for the mass ratio r generated by the HHG. In the plots the generator is used in a) 1-P mode, b) 2-P mode with $P_s = 500$ kPa, and c) in divided-flow mode.

8. Comparisons with other Humidity Standards

8.1. NIST Gravimetric Hygrometer

We have performed comparisons between the humidity generated by the HHG and that measured by the NIST gravimetric hygrometer [18,19]. The gravimetric hygrometer is a primary standard for humidity measurement. It determines the mass ratio of water to air in a humid gas sample by separating out the water from the gas and subsequently determining the masses of the water and dry air. The results of the comparison are shown in Figure 26, which plots $\Delta x/x$, where $\Delta x \equiv x_{GH} - x_{HHG}$; here, x_{GH} is the water amount fraction measured by the gravimetric hygrometer and x_{HHG} is that generated using the HHG. Here, the saturator pressure was ≈ 200 kPa for all points except for those where $\log_{10}(x) = -2.7$. In this case, the saturator pressure was 300 kPa and the saturator temperature was 1 °C; these are the saturator parameters used when the HHG is operated in divided-flow mode.

The expanded uncertainty ($k = 2$) of the amount fraction measurements by the gravimetric hygrometer is estimated to be 0.20 % over the range of humidity in the plot. For the hybrid generator using the above parameters, the expanded uncertainty is estimated to be less than 0.08 %, so the combined expanded relative uncertainty of the HHG and gravimetric hygrometer is estimated to be $U_r(x) \approx 0.22$ %.

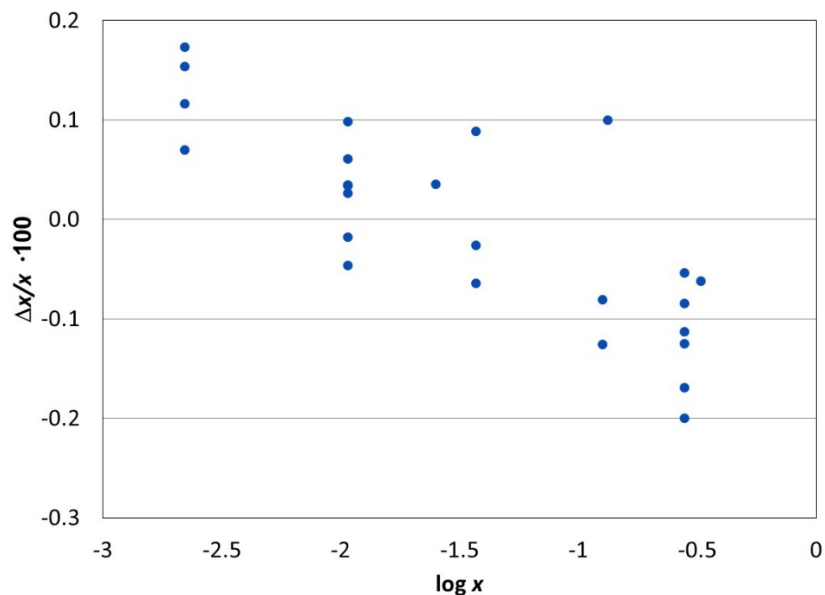


Figure 26. Comparison of water amount fraction x measured by the NIST gravimetric hygrometer with that generated by the HHG. Here, $\Delta x \equiv x_{GH} - x_{HHG}$, where x_{GH} is the amount fraction measured by the gravimetric hygrometer and x_{HHG} is that generated using the HHG. The combined expanded ($k = 2$) relative uncertainties of the gravimetric hygrometer and generator are $U_r(x) \approx 0.22$ %.

The values of $\Delta x/x$ are all within 0.2 % and the averages of the points taken at one value of x are all within 0.12 %. This is within the combined uncertainties of the HHG and gravimetric hygrometer, showing agreement between the two systems.

8.2. CCT Key Comparisons

Under the Mutual Recognition Arrangement (MRA) [20] it was agreed that the metrological equivalence of national measurement standards would be determined by a set of key comparisons chosen and organized by the consultative committees of the International Committee for Weights and Measures (CIPM) working closely with the Regional Metrology Organizations (RMOs).

In 2001 the Consultative Committee for Thermometry (CCT) of the CIPM arranged for a multilateral key comparison of dew/frost-point standards, named CCT-K6 [21], with the National Physical Laboratory (NPL, UK) to be its pilot and the National Measurement Institute of Japan (NMIJ, Japan) to be its co-pilot. The assigned participants were the National Metrology Institutes (NMIs) of the UK, Japan, the United States, Finland, Spain, Italy, China, Singapore, Russia, and the Netherlands. The comparison points were 20 °C, 1 °C, -10 °C, -30 °C, and -50 °C. The comparison measurements were performed between 2002 and 2009. As the NMI of the United States, NIST participated in the comparison, performing its measurements in 2007. It used the HHG as its standard at the points 20 °C, 1 °C, and -10 °C. At the time of these measurements, the divided-flow system for the HHG was not yet operational, so NIST used its Low Frostpoint Generator (LFPG) [22] (now decommissioned) as its standard at the points -30 °C and -50 °C.

The comparison measurements by all participants were performed using two chilled-mirror hygrometers supplied by the pilots, called transfer standards. Each NMI used its primary standard generator to produce humid air with a dew/frost-point $T_{\text{DP/FP}}^g$. It then used the transfer standards to obtain the measured dew/frost-point $T_{\text{DP/FP}}^m$. The difference between the two, $\Delta T_{\text{DP/FP}}$, given by

$$\Delta T_{\text{DP/FP}} = T_{\text{DP/FP}}^g - T_{\text{DP/FP}}^m, \quad (18)$$

was the quantity used to compare the dew/frost-point standards of the participants in the key comparison.

One of the achievements of CCT-K6 was the creation of key comparison reference values (KCRVs) for $\Delta T_{\text{DP/FP}}$ at the comparison points [21], $[\Delta T_{\text{DP/FP}}]_{\text{KCRV}}$. These KCRVs are considered to be international consensus values for dew/frost-point standards at these points. They are also reference values with which all NMIs can establish degrees of equivalence. If NMI standards have established degrees of equivalence (DoE's) to the KCRVs, they can establish DoE's with each other without performing direct comparison measurements. By participating in CCT-K6, the HHG has established DoE's to the CCT-K6 KCRVs. For a given NMI, the DoE $D_{\text{NMI/KCRV}}$ at a dew/frost-point temperature $T_{\text{DP/FP}}$, is given by

$$D_{\text{NMI/KCRV}}(T_{\text{DP/FP}}) \equiv [\Delta T_{\text{DP/FP}}]_{\text{NMI}} - [\Delta T_{\text{DP/FP}}]_{\text{KCRV}}. \quad (19)$$

In Table 2, the DoE's between the HHG dew/frost-point standards and the KCRVs are shown, along with their expanded ($k = 2$) uncertainties (obtained from Tables 7.3 and 7.4 in [21]). The DoE values are well within their expanded ($k = 2$) uncertainties.

Table 2. Degree of equivalence between $T_{DP/FP}$ realized by NIST and the KCRV, $D_{NIST/KCRV}$, and its expanded uncertainty ($k = 2$), $U(D_{NIST/KCRV})$, at $T_{DP/FP}$ values of 20 °C, 1 °C, and -10 °C, as given by Tables 7.3 and 7.4 in [21].

Nominal $T_{DP/FP}$ (°C)	$D_{NIST/KCRV}$ (°C)	$U(D_{NIST/KCRV})$ (°C)
20	-0.006	0.050
1	-0.011	0.060
-10	-0.039	0.043

Because the HHG wasn't involved with the 2007 comparison measurements at -30 °C and -50 °C for CCT-K6, NIST later used the HHG to perform a bilateral comparison with the National Metrology Institute of Japan, of the National Institute of Advanced Industrial Science and Technology (NMIJ/AIST, Japan), designated CCT-K6.2, at these two frost points as well as at -70 °C and -80 °C [23]. The measurements were performed between December 2015 and November 2016. The results of the comparison directly established the DoE between NIST HHG and NMIJ/AIST frost-point standards at these points. They also indirectly established the DoE between the NIST HHG frost-point standards and the CCT-K6 KCRVs at these points, since NMIJ provided linkage through its participation in that key comparison. In Table 3, the DoE's between the HHG dew/frost-point standards and the KCRVs are shown, along with their expanded ($k = 2$) uncertainties. Here, the DoE values are also well within their expanded uncertainties. Note that the uncertainties in Table 3 are higher than those of Table 2 because the DoE has been established indirectly.

Table 3. Degree of equivalence between T_{FP} realized by NIST and the KCRV, $D_{NIST/KCRV}$, and its expanded uncertainty ($k = 2$), $U(D_{NIST/KCRV})$, at T_{FP} values of -30 °C and -50 °C, as determined by the bilateral comparison CCT-K6.2 [23] between NIST and NMIJ/AIST (Japan).

Nominal $T_{DP/FP}$ (°C)	$D_{NIST/KCRV}$ (°C)	$U(D_{NIST/KCRV})$ (°C)
-30	-0.048	0.075
-50	-0.012	0.142

Although there are no CCT-K6 KCRVs at $-70\text{ }^{\circ}\text{C}$ and $-80\text{ }^{\circ}\text{C}$, it is nevertheless useful to show the DoE between the NIST HHG and NMIJ/AIST standards at those point for validation of their standards. The DoE values and their expanded uncertainties are shown in Table 4. The DoE values are well within the expanded uncertainties, showing agreement between the standards of NIST and NMIJ/AIST at these points.

Table 4. Degree of equivalence between T_{FP} realized by NMIJ/AIST (Japan) and that of NIST, and its expanded uncertainty ($k = 2$) at $-70\text{ }^{\circ}\text{C}$ and $-80\text{ }^{\circ}\text{C}$.

Nominal $T_{\text{DP/FP}}$ ($^{\circ}\text{C}$)	$D_{\text{NIST/NMIJ}}$ ($^{\circ}\text{C}$)	$U(D_{\text{NIST/NMIJ}})$ ($^{\circ}\text{C}$)
-70	-0.045	0.466
-80	0.059	0.112

In 2008, the CCT arranged for a multilateral key comparison of above-ambient dew-point standards, named CCT-K8 [24], with the Instituto Nacional de Técnica Aeroespacial (INTA, Spain) as its pilot and NIST as its co-pilot. The additional participants were KRISS (South Korea), (NMC-A*STAR (Singapore), NMIJ/AIST (Japan), VNIIFTRI (Russia), INRiM (Italy), NPL (UK), PTB (Germany), and BEV/E+E (Austria). Measurements were made in 2016 and 2017. The comparisons were made at dew point temperatures of $30\text{ }^{\circ}\text{C}$, $50\text{ }^{\circ}\text{C}$, $65\text{ }^{\circ}\text{C}$, $80\text{ }^{\circ}\text{C}$, $85\text{ }^{\circ}\text{C}$, $90\text{ }^{\circ}\text{C}$, and $95\text{ }^{\circ}\text{C}$. As the NIST HHG does not realize dew points above $85\text{ }^{\circ}\text{C}$, it did not perform comparison measurements at $90\text{ }^{\circ}\text{C}$ and $95\text{ }^{\circ}\text{C}$. At the time of this writing, Draft A of the CCT-K8 report is still in progress.

8.3. SIM Key Comparisons

The NIST HHG has participated in a number of bilateral comparisons for the Inter-American Metrology System (SIM), the Regional Metrology Organization (RMO) for North, Central, and South America. It has performed comparisons with NRC (Canada) from $-25\text{ }^{\circ}\text{C}$ to $20\text{ }^{\circ}\text{C}$ (designated SIM.T-K6.1) [25], CENAM (Mexico) from $-20\text{ }^{\circ}\text{C}$ to $20\text{ }^{\circ}\text{C}$ (designated SIM.T-K6.2) [26], INMETRO (Brazil) from $-30\text{ }^{\circ}\text{C}$ to $20\text{ }^{\circ}\text{C}$ (designated SIM.T-K6.3) [27], and LACOMET (Costa Rica) from $-30\text{ }^{\circ}\text{C}$ to $20\text{ }^{\circ}\text{C}$ (designated SIM.T-K6.5) [28]. All comparisons have shown DoE's within the expanded uncertainties, showing agreement between the standards of NIST and the above-mentioned NMIs at these points. These comparisons have made it possible for these SIM NMIs to establish the DoE's between their dew/frost-point standards and the CCT-K6 KCRVs at several points.

9. Calibration of Chilled-Mirror Hygrometers and Cavity Ringdown Spectrometers

9.1. Initial Procedures

Before connecting the hygrometers to the hybrid generator, they are checked for noticeable damage and for proper operation. Any damage or serious operation problems is grounds for rejecting the instrument for calibration. For the case of chilled-mirror hygrometers, we clean the hygrometer mirrors first with ethanol and afterwards with distilled water. Finally, tests are performed to ensure that calibration points requested for each hygrometer are within its measurement range.

9.2. Connecting the Hygrometers to the Hybrid Generator

The manifold connecting the hygrometers to the generator is shown in Fig. 27. A maximum of two customer hygrometers can be connected to the generator. Normally only one hygrometer is attached for a calibration, but if a customer sends two hygrometers and requests the same calibration points, the manifold can accommodate simultaneous calibrations. The manifold includes bypass tubes that lead out to the room. Each bypass tube has an adjustable valve that allows control of the flow rate of output gas entering the hygrometers. As shown in the figure, a pressure gauge is located near the input to the first customer hygrometer for measuring the pressure of the customer hygrometers and check standard.

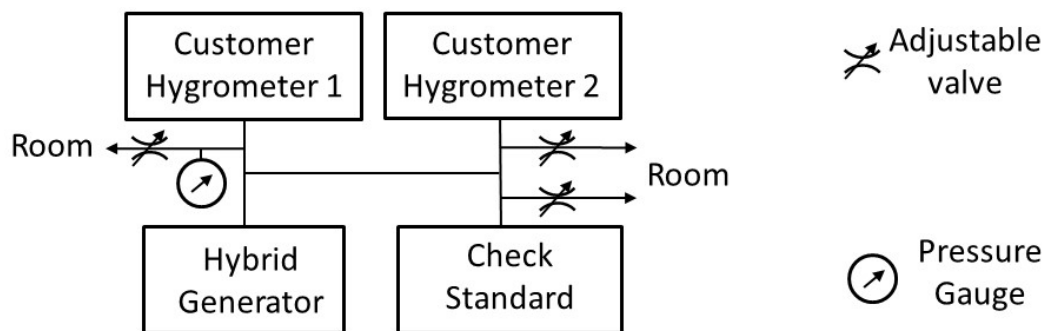


Figure 27. Connections of customer hygrometer and check standard to hybrid generator.

If the desired humidity values exceed a frost point of $-10.3\text{ }^{\circ}\text{C}$ ($x = 2.3 \times 10^{-3}$), the hygrometers are connected directly to the output of the 2-P generator, at a point downstream of the expansion valve, as shown in Figure 1a. If the desired dew-point values are above ambient temperature, the tubes connecting the output of the generator to the hygrometers are wrapped with heater tape so that they can be heated to at least $30\text{ }^{\circ}\text{C}$ above the generated dew-point temperature.

If the desired humidity values are below a frost point of $-10.3\text{ }^{\circ}\text{C}$, the divided-flow system is used, with the multiplexer attached to the saturator. The hygrometers are attached to the output of the multiplexer, as shown in Fig. 1b.

The tubing used for connecting the generator to the hygrometers is made of electropolished stainless steel. The valves and fittings used in the manifold are also made of stainless steel. The fittings are almost always of the metal-gasket face-seal type. The exceptions are at the customer hygrometer input when it has a compression fitting and for the connections to the adjustable valves.

9.3. Calibration Measurements

The calibrations are done at specific humidity points as requested by the customer. The order in which the calibration points are acquired is at the discretion of the operator. However, for highest efficiency we plan the order so that as many points as possible can be taken at one saturator temperature.

The hybrid generator temperature/pressure parameters are set to generate the desired humidity. The flow rate through each hygrometer is set to that recommended by the instrument manufacturer (typically 0.5 L/min). After setting the hybrid generator to produce the desired humidity, a computer application opens up a spreadsheet. For each nominal humidity point, a data-acquisition application commands the relevant instruments to measure the temperature and pressure of the saturator, the pressure of the air entering the hygrometers, and the wet-gas and dry-gas flows (if the divided flow method is used); these measurements are used to calculate x and $T_{DP/FP}$ inside the hygrometers using Eqs. 1-3. For each set of measurements, the application also records the x or $T_{DP/FP}$ measurement of the customer hygrometer and check standard hygrometer. All measurements are recorded in a spreadsheet at 30 s intervals for at least 30 min after all measurements reach a steady state. Finally, the application averages the measurements for the last 30 min to give the final values. If the readings never reach a steady state, efforts will be made to find and fix the source of the problem. The spreadsheet includes plots that monitor the saturator temperature and pressure, as well as the dew/frost point and molar fraction of the generator. It also includes plots that monitor the measurements of the check standard and customer hygrometers.

Once the data is acquired for all requested humidity points, the results are assembled into a workbook. The new check standard data is compared to previous check standard data to validate the performance of the generator during this set of measurements. The final results comparing the customer hygrometer humidity to the HHG humidity are placed in a calibration report similar to that shown in Appendix III. For calibrations of chilled-mirror hygrometers measuring relative humidity, dew-point calibrations are made using the generator while a comparison calibration is made of the temperature probe against a reference thermometer in a stirred bath [15]. The reference relative humidity is calculated using the generated value of x and reference temperature values using Eq. 4.

If the stability and/or repeatability of the hygrometer are significantly worse than the values given by the hygrometer specifications and the sources of these problems cannot be corrected, the hygrometer is rejected for calibration and returned to the customer.

As a check on the consistency of the HHG, a check standard (a chilled-mirror hygrometer) is attached to the output of the generator as shown in Fig. 27 when performing calibrations. A measurement history of the check standard exists for dew/frost points at available multiples of 10 °C (i.e. -70 °C, -60 °C, ... 70 °C, 80 °C) as well as 85 °C. During a hygrometer calibration, comparisons are made of the check-standard points with their historical values. Data acquisition for the check standard is performed as described in section 9.4. If the new check standard measurements differ from the average of the old measurements by more than the expanded total uncertainty ($k=2$) of the HHG and hygrometer, the new results are considered suspect, and further investigation must be made to determine the validity of these results. An example of a check-standard history plot is shown in Fig. 28. The standard deviation of the points in the plot is 20 mK.

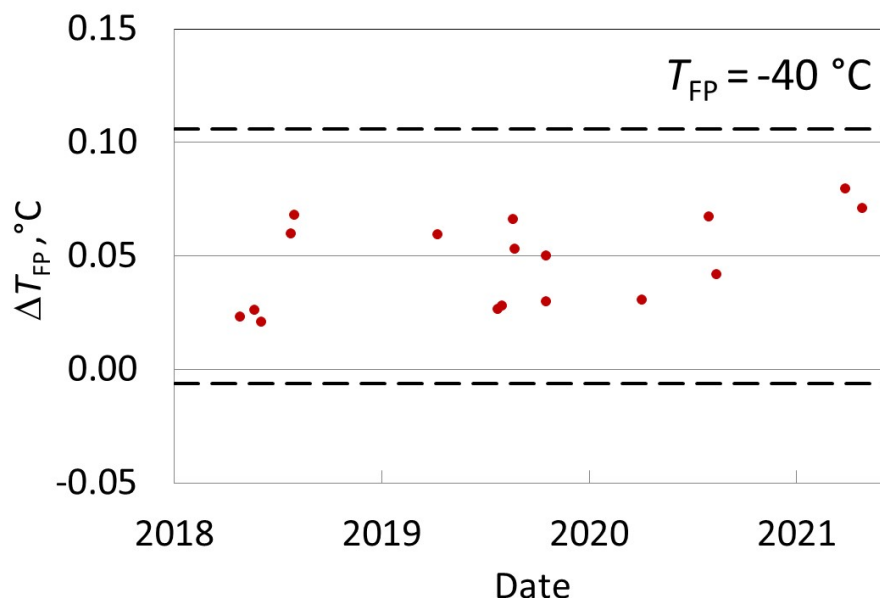


Figure 28. Check Standard history plot for a frost point of $-40\text{ }^{\circ}\text{C}$. The plot shows the difference ΔT_{FP} between the frost-point temperature measured by the check standard and that generated by the HHG as a function of date. The dashed lines represent the $k = 2$ uncertainty limits for the hygrometer repeatability. The standard deviation of the points in the plot is 20 mK.

10. Calibration of Thermohygrometers and Dataloggers

10.1. Initial Procedures

Before beginning calibration of the thermohygrometers and dataloggers, they are checked for noticeable damage and for proper operation. Any sign of damage or serious operation problems is grounds for rejecting an instrument for calibration.

The instrument sensors are calibrated in the HHG test chamber (see section 6). For instruments with a cord between their sensor and controller, the sensor is placed inside the chamber while the controller is placed outside the environmental chamber. The cord enters the side of the environmental chamber between a square opening and a slightly compressible square cork block that seals the opening. The cord enters the test chamber from the environmental chamber through a circular port of diameter 2.2 cm. A thermohygrometer with a sensor that has a diameter larger than 2.2 cm cannot be calibrated using this configuration; in this case the controller may need to be placed in the test chamber as well.

The test chamber does not have a window allowing visual observation of the items inside. Therefore, if the controller must be placed inside the chamber, it must provide some means for data communications with a computer located outside the environmental chamber (e.g. a RS-232 serial port). The communications need not be simultaneous with the instrument measurements. For

example, with dataloggers, where the controller and sensors are together in one unit, the measurement values can be transmitted after the measurements are completed and the datalogger is taken out of the test chamber.

Instrument sensors are generally placed near the center of the chamber and as close to the test chamber reference thermometer as possible to minimize temperature differences between them. This arrangement is shown in Fig. 14; however, in this photograph the customer instrument (a datalogger) was placed further away than normal for ease of viewing. The sensors are usually mounted by attaching them to a vertical rod in the chamber using a cable tie, as shown in the lower photograph of Fig. 14. If multiple dataloggers are calibrated in the chamber simultaneously, they may be placed on a horizontal metal grill mounted in the chamber at about 1/3 the height of the chamber.

Once the instrument sensors are placed in the test chamber, the environmental chamber is set to control at the desired temperature for the calibration measurement. Additionally, the heat exchanger between the HHG output and the environmental chamber (see section 6.2) is set to control at this same temperature. If the desired relative humidity value corresponds to a dew/frost point that exceeds $-10.3\text{ }^{\circ}\text{C}$ ($x = 2.3 \times 10^{-3}$), the heat exchanger is connected directly to the output of the 2-P generator, immediately downstream of the PID throttle valve shown in Fig. 1a. If the relative humidity corresponds to a dew point above ambient temperature, the tubes connecting the throttle valve to the heat exchanger are wrapped with heater tape so that they can be heated to at least $30\text{ }^{\circ}\text{C}$ above the generated dew-point temperature. If the desired relative humidity value corresponds to a frost point at or below $-10.3\text{ }^{\circ}\text{C}$, the divided-flow system is used, with the multiplexer attached to the saturator. The heat exchanger is attached to the output of the multiplexer shown in Fig. 1b.

10.2. Calibration Measurements

The calibrations are done at specific temperature and relative humidity points as requested by the customer. The order in which the calibration points are acquired is at the discretion of the operator. However, for highest efficiency we plan the order so that as many points as possible can be taken at one saturator and/or chamber temperature.

The hybrid generator temperature/pressure parameters are set to generate the desired relative humidity for the given chamber temperature. The flow rate through the chamber is set to 150 L/min. Afterwards, a computer application opens up a spreadsheet. For each nominal relative humidity point, a data-acquisition application commands the relevant instruments to measure the temperature and pressure of the saturator, the pressure of the air entering the test chamber, the wet-gas and dry-gas flows (if the divided-flow method is used), and the temperature inside the test chamber; these measurements are used to calculate RH and $T_{DP/FP}$ inside the test chamber using Eqs. 2-4. For each set of measurements, the application also records RH using a thermohygrometer check standard and $T_{DP/FP}$ using a chilled-mirror check standard. All measurements are recorded in a spreadsheet at 90 s intervals for at least 30 min after all measurements reach a steady state. Finally, the application averages the measurements for the last 30 min to give the final values. If the readings never reach a steady state, efforts will be made to find and fix the source of the problem. The spreadsheet includes plots that monitor the saturator temperature and pressure, as well as the relative humidity and dew/frost point in the test chamber. It also includes plots that monitor the measurements of the check standards and customer instruments.

Once the data is acquired for all requested humidity points, the results are assembled into a workbook. The new check standard data is compared to previous check standard data to validate the performance of the generator during this set of measurements. The final results comparing the customer instrument's temperature and relative humidity measurements to the HHG test chamber temperature and relative humidity are placed in a calibration report similar to that shown in Appendix III.

11. Quality Control

The pressure gauges used for measuring the pressure in the saturator and the hygrometer are recalibrated against a piston gauge by the NIST Thermodynamic Metrology Group once every two years. The SPRT used for measuring the saturator temperature is checked yearly against the water triple point and the PRTs used for measuring the test chamber, environmental chamber, and heat exchanger temperatures are checked yearly against the ice point. The respective R_0 values of the SPRT and PRTs are adjusted to conform with the results of these measurements. For the SPRT and test chamber PRT, if the temperature measurement at this point differs by more than 10 mK from that of the original calibration, the thermometer is recalibrated over its full range by the NIST Thermodynamic Metrology Group. The SPRT's bridge and resistance standard are also checked on a periodic basis. The laminar flow elements used for measuring the wet and dry flow in the divided flow system are also recalibrated periodically.

NIST is a self-accrediting body that conforms to ISO/IEC 17025 quality standards [29]. The NIST humidity calibration services undergo 17025 conformity assessments every two years by assessors within NIST but outside of the NIST Thermodynamic Metrology Group.

12. Summary

We have described here the design and performance of the NIST hybrid generator, which generates dew/frost points between $-90\text{ }^{\circ}\text{C}$ and $85\text{ }^{\circ}\text{C}$ (amount fractions between $0.1\text{ }\mu\text{mol/mol}$ and 0.57 mol/mol). This primary generator uses a novel design that incorporates both the two-pressure method and divided-flow method. Between $-70\text{ }^{\circ}\text{C}$ and $85\text{ }^{\circ}\text{C}$, the dew/frost-point expanded uncertainty is always below 25 mK. As the frost point decreases from $-70\text{ }^{\circ}\text{C}$ to $-90\text{ }^{\circ}\text{C}$, the uncertainty increases from 25 mK to 120 mK due to the increasing influence of the uncertainty of x_p , which we estimate to be $u(x_p) = 1\text{ nmol/mol}$. Over the low frost-point range, this uncertainty is considerably lower than the uncertainty of most 2-P generators. Comparison of the expected humidity generated by the HHG with that measured by the NIST gravimetric hygrometer shows agreement within the combined expanded uncertainties of the generator and hygrometer. Key comparisons of the humidity generated by the HHG with that of humidity generators of other major NMIs shows agreement within the expanded uncertainties of the generators and transfer standard. These comparisons provide a satisfactory validation of the performance of the HHG.

We have also described the design and performance of the NIST HHG test chamber. This chamber, when combined with the HHG, can calibrate thermohygrometers and dataloggers over the range 2 % to 98 % for temperatures between $-34\text{ }^{\circ}\text{C}$ and $85\text{ }^{\circ}\text{C}$. The expanded relative uncertainty of the relative humidity in this system is less than 0.3 %.

Acknowledgements

The authors thank Dr. Joseph T. Hodges for conceiving the humidity generator described in this document, obtaining the funding to develop it, and performing preliminary calculations on its performance. The authors also thank Gregory E. Scace for his many contributions to the development of this generator, including the design of the HHG final saturator, test chamber, and the test chamber heat exchanger.

References

- [1] G.E. Scace et al., “An Overview of the NIST Hybrid Humidity Generator”, in Proceedings of the 5th International Symposium on Humidity and Moisture (Rio de Janeiro, Brazil: INMETRO, 2007).
- [2] C.W. Meyer et al., “Performance and Validation Tests on the NIST Hybrid Humidity Generator”, in Proceedings of the 10th International Symposium on Temperature and Thermal Measurements in Industry and Science (TEMPMEKO 2007), *Int. J. Thermophys.* **29**, 1606–1614 (2008).
- [3] C.W. Meyer et al., “Uncertainty Budget for the NIST Hybrid Humidity Generator”, in Proceedings of the 11th International Symposium on Temperature and Thermal Measurements in Industry and Science (TEMPMEKO 2010), *Int. J. Thermophys.* **33**, 1488–1499 (2012).
- [4] W. Wagner and A. Pruss, “International Equations for the Saturation Properties of Ordinary Water Substance--Revised According to the International Temperature Scale of 1990”, *J. Phys. Chem. Ref. Data* **22**, 783–787 (1993).
- [5] R.W. Hyland and A. Wexler, “Formulations for the Thermodynamic Properties of Dry Air from 173.15 K to 473.15 K, and of Saturated Moist Air from 173.15 K to 372.15 K, at Pressures to 5 MPa.”, *ASHRAE Trans.* **89-IIa**, 520–535 (1983).
- [6] A. Wexler, “Humidity Standards”, *Tappi* **44** (6), 180A –191A (1961).
- [7] J. W. Lovell-Smith et al., “Metrological challenges for measurements of key climatological observables. Part 4: atmospheric relative humidity”, *Metrologia* **53**, R40–R59, (2016).
- [8] International Association for the Properties of Water and Steam, R14-08(2011), “Revised Release on the Pressure along the Melting and Sublimation Curves of Ordinary Water Substance” (2011), available at www.iapws.org.
- [9] W. Wagner et al., “New Equations for the Melting Pressure and Sublimation Pressure of H₂O Ice Ih”, *J. Phys. Chem. Ref. Data.* **40**, 043103 (2011).
- [10] International Association for the Properties of Water and Steam, G5-01(2020), “Guideline on the Use of Fundamental Physical Constants and Basic Constants of Water” (2020), available at www.iapws.org.
- [11] A. Picard et al., “Revised formula for the density of moist air (CIPM-2007)”, *Metrologia* **45**, 149 (2008).
- [12] ASTM Standard E 1137/E 1137M - 08, “Standard Specification for Industrial Platinum Resistance Thermometers”, Annual Book of ASTM Standards, vol. 14.03, ASTM International, Conshohocken, PA (2020).

- [13] BIPM, IEC, IFCC, ILAC, ISO, IUPAC, IUPAP and OIML, “Evaluation of measurement data--Guide to the expression of uncertainty in measurement”, JCGM 100:2008, https://www.bipm.org/utis/common/documents/jcgm/JCGM_100_2008_E.pdf, (2008).
- [14] B.N. Taylor and C.E. Kuyatt, “Guidelines for Evaluating and Expressing the Uncertainty of NIST Measurement Results”, NIST Technical Note 1297, National Institute of Standards and Technology, Gaithersburg (1994).
- [15] C.D. Vaughn and G.F. Strouse, “The NIST Industrial Thermometer Calibration Laboratory”, in *Proceedings of TEMPMEKO 2001: the 8th International Symposium on Temperature and Thermal Measurements*, B. Fellmuth, J. Seidel, G. Scholz, eds., VDE Verlag GMBH, Berlin (2002), 629-634.
- [16] W. Wagner and A. Pruss, “The IAPWS Formulation 1995 for the Thermodynamic Properties of Ordinary Water Substance for General and Scientific Use”, *J. Phys. Chem. Ref. Data* **31**, 387 (2002).
- [17] R.W. Hyland, “A Correlation for the Second Interaction Virial Coefficients and Enhancement Factors for Moist Air”, *J. Res. NBS* **79A**, 551–560 (1975).
- [18] C.W. Meyer et al., “Automated Continuous-Flow Gravimetric Hygrometer as a Primary Humidity Standard”, in *Proceedings of the 5th International Symposium on Humidity and Moisture*, (Rio de Janeiro, Brazil: INMETRO, 2007).
- [19] C.W. Meyer, et al., “The Second-generation NIST Standard Hygrometer”, *Metrologia* **47** 192 (2010).
- [20] CIPM MRA Documents, <https://www.bipm.org/en/cipm-mra/cipm-mra-documents>.
- [21] S. Bell et al., CCT-K6 Final Report, NPL REPORT ENG 57, *Metrologia* **52**, Tech. Suppl., 03005 (2015).
- [22] G.E. Scace and J.T. Hodges, “Uncertainty of the NIST Low Frost-point Humidity Generator”, in *Proceedings of TEMPMEKO 2001: the 8th International Symposium on Temperature and Thermal Measurements*, B. Fellmuth, J. Seidel, G. Scholz, eds., VDE Verlag GMBH, Berlin (2002), 597-602.
- [23] C.W. Meyer and H. Abe, CCT-K6.2 Final Report, *Metrologia* **57** Tech. Suppl. 03007 (2020).
- [24] CCT-K8 Technical Protocol, <https://www.bipm.org/kcdb/comparison?id=1073>.
- [25] C.W. Meyer and K.D. Hill, SIM.T-K6.1 Final Report, *Metrologia* **52** Tech. Suppl., 03008 (2015).

- [26] P.H. Huang et al., SIM.T-K6.2 Final Report, *Metrologia* **51** Tech. Suppl., 03002 (2014)
- [27] P. Huang, C. Meyer, and J.D. Brionizio, SIM.T-K6.3 Final Report, *Metrologia* **52** Tech. Suppl., 03001 (2015)
- [28] C. W. Meyer, and A. Solano, SIM.T-K6.5 Final Report, *Metrologia* **53** Tech. Suppl., 03005 (2016)
- [29] ISO/IEC, General Requirements for the Competence of Testing and Calibration Laboratories, ISO/IEC 17025:2017 (2017).
- [30] J.W. Lovell-Smith, “On Correlation in the Water Vapour Pressure Formulation”, *Metrologia* **43**, 556 (2006).

Appendix I. Derivation of the Uncertainty Equations for the Hybrid Generator

The total uncertainty of a quantity z is related to the n individual uncertainty components y_i through the general law of error propagation [12]:

$$u(z)^2 = \sum_{i=1}^n \left(\frac{\partial z}{\partial y_i} \right)^2 u(y_i)^2 + 2 \sum_{i=1}^{n-1} \sum_{j=i+1}^n r_{i,j} \frac{\partial z}{\partial y_i} \frac{\partial z}{\partial y_j} u(y_i) u(y_j) \quad A1)$$

The relevant quantities and the derivatives $\partial z/\partial y_i$ may be found by expanding the differential dz :

$$dz = \sum_{i=1}^n \frac{\partial z}{\partial y_i} dy_i. \quad A2)$$

Below, the total uncertainty for humidity generated by the hybrid generator will be derived for four cases: 1) water amount fraction when the generator is used in 2-P mode or 1-P mode, 2) dew-point temperature when the generator is used in 2-P mode or 1-P mode, 3) water amount fraction when the generator is used in divided-flow mode, and 4) frost-point temperature when the generator is used in divided-flow mode.

1. Water Amount Fraction When the Generator is Used in 2-P Mode or 1-P Mode

The total uncertainty for this case is obtained by applying Eq. A2 to Eq. 1, which yields

$$dx = \frac{f_s}{P_s} de_s + \frac{e_s}{P_s} df_s - \frac{e_s f_s}{P_s^2} dP_s. \quad A3)$$

where $f_s \equiv f(T_s, P_s)$ and $e_s \equiv e(T_s, P_s)$. In de_s , we can separate out the differential relating to the uncertainty of its calculating equation de_s^{calc} from that relating to the uncertainty of the temperature from which it is calculated:

$$de_s = de_s^{\text{calc}} + \frac{de_s}{dT_s} dT_s. \quad A4)$$

Similarly, in df_s , we can separate out to the differential relating to the uncertainty of its calculating equation df_s^{calc} from that relating to the uncertainty of the temperature and pressure from which it is calculated:

$$df_s = df_s^{\text{calc}} + \frac{df_s}{dT_s} dT_s + \frac{df_s}{dP_s} dP_s. \quad A5)$$

However, because df_s/dT_s and df_s/dP_s are very small, Eq. A5 may be approximated as $df_s \approx df_s^{\text{calc}}$. Using this approximation while combining Eqs. A3–A4 gives

$$dx = \frac{f_s}{P_s} \frac{de_s}{dT_s} dT_s - \frac{e_s f_s}{P_s^2} dP_s + \frac{f_s}{P_s} de_s^{\text{calc}} + \frac{e_s}{P_s} df_s^{\text{calc}}. \quad \text{A6)}$$

The uncertainty in the amount fraction may then be expressed as

$$u(x)^2 = \left(\frac{f_s}{P_s} \frac{de_s}{dT_s} \right)^2 u(T_s)^2 + \left(\frac{e_s f_s}{P_s^2} \right)^2 u(P_s)^2 + \left(\frac{f_s}{P_s} \right)^2 u(e_s^{\text{calc}})^2 + \left(\frac{e_s}{P_s} \right)^2 u(f_s^{\text{calc}})^2, \quad \text{A7)}$$

and the relative uncertainty $u_r(x)$ is then given by

$$u_r(x)^2 = \left[\frac{u(x)}{x} \right]^2 = \left(\frac{1}{e_s} \frac{de_s}{dT_s} \right)^2 u(T_s)^2 + \frac{u(P_s)^2}{P_s^2} + \frac{u(e_s^{\text{calc}})^2}{e_s^2} + \frac{u(f_s^{\text{calc}})^2}{f_s^2}. \quad \text{A8)}$$

2. Dew-point Temperature When the Generator is Used in 2-P Mode or 1-P Mode

Here we consider the total uncertainty for the dew-point temperature T_{DP} in a chamber with temperature $T_c = T_{\text{DP}}$, pressure P_c , and water vapor pressure e_c . This uncertainty may be determined by inverting Eq. A4 to solve for dT_s and then substituting the saturator parameters with the chamber parameters (T_s with T_{DP} , e_s with e_c , and e_s^{calc} with e_c^{calc}):

$$dT_{\text{DP}} = dT_c = \frac{1}{[de_c / dT_{\text{DP}}]} (de_c - de_c^{\text{calc}}). \quad \text{A9)}$$

Letting $f_c \equiv f(T_c, P_c)$, we can express e_c in terms of x and P_c :

$$e_c = \frac{xP_c}{f_c}. \quad \text{A10)}$$

Differentiating Eq. A10 and inserting the resulting expression for de_c in Eq. A9 gives

$$dT_{\text{DP}} = \frac{1}{[de_c / dT_{\text{DP}}]} \left[\frac{P_c}{f_c} dx + \frac{x}{f_c} dP_c - \frac{xP_c}{f_c^2} df_c - de_c^{\text{calc}} \right]. \quad \text{A11)}$$

Using the approximation $df_c \cong df_c^{\text{calc}}$ in Eq. A11 and combining it with Eqs. 1 and A6 and yields

$$dT_{\text{DP}} = \frac{1}{[de_c / dT_c]} \left[\frac{P_c f_s}{P_s f_c} \frac{de_s}{dT_s} dT_s - \frac{P_c e_s f_s}{P_s^2 f_c} dP_s + \left(\frac{P_c f_s}{P_s f_c} de_s^{\text{calc}} - de_c^{\text{calc}} \right) + e_c \left(\frac{e_s P_c}{P_s f_c} df_s^{\text{calc}} - \frac{df_c^{\text{calc}}}{f_c} \right) + \frac{e_c}{P_c} dP_c \right]. \quad \text{A12)}$$

Recognizing that x is the same in both the saturator and chamber, $e_s f_s / P_s = e_c f_c / P_c$, and so A12 may be written

$$dT_{DP} = \frac{e_c}{[de_c / dT_{DP}]} \left[\frac{1}{e_s} \frac{de_s}{dT_s} dT_s - \frac{dP_s}{P_s} + \left(\frac{de_s^{\text{calc}}}{e_s} - \frac{de_c^{\text{calc}}}{e_c} \right) + \left(\frac{df_s^{\text{calc}}}{f_s} - \frac{df_c^{\text{calc}}}{f_c} \right) + \frac{dP_c}{P_c} \right]. \quad \text{A13)}$$

This equation can be simplified by defining the differentials

$$d\Delta e^{\text{calc}} \equiv \frac{de_s^{\text{calc}}}{e_s} - \frac{de_c^{\text{calc}}}{e_c} \quad \text{and} \quad \text{A14)}$$

$$d\Delta f^{\text{calc}} \equiv \frac{df_s^{\text{calc}}}{f_s} - \frac{df_c^{\text{calc}}}{f_c}. \quad \text{A15)}$$

Then Eq. A13 becomes

$$dT_{DP} = \frac{e_c}{[de_c / dT_{DP}]} \left[\frac{1}{e_s} \frac{de_s}{dT_s} dT_s - \frac{dP_s}{P_s} + d\Delta e^{\text{calc}} + d\Delta f^{\text{calc}} + \frac{dP_c}{P_c} \right]. \quad \text{A16)}$$

And the uncertainty of the dew-point temperature is

$$u(T_{DP})^2 = \left(\frac{e_c}{[de_c / dT_{DP}]} \right)^2 \left[\left(\frac{1}{e_s} \frac{de_s}{dT_s} \right)^2 u(T_s)^2 + \frac{u(P_s)^2}{P_s^2} + \frac{u(P_c)^2}{P_c^2} + u_r(\Delta e^{\text{calc}})^2 + u_r(\Delta f^{\text{calc}})^2 \right] \quad \text{A17)}$$

The relative uncertainties $u_r(\Delta f^{\text{calc}})$ and $u_r(\Delta e^{\text{calc}})$ have not been resolved by the humidity community, and it is currently an area of active work [30]. Because of this, we use in this document the conventional analysis [30]. When the generator is used in 1-P mode ($P_s \cong P_c$), this method assumes that $e_c \cong e_s$ and $f_c \cong f_s$, and therefore

$$u_r(\Delta e^{\text{calc}}) = u_r(\Delta f^{\text{calc}}) = 0 \quad \text{A18)}$$

For the 2-P mode ($P_s \neq P_c$), the method assumes that there are no correlations between $u(e_s^{\text{calc}})$ and $u(e_c^{\text{calc}})$ and between $u(f_s^{\text{calc}})$ and $u(f_c^{\text{calc}})$; therefore

$$u_r(\Delta e^{\text{calc}})^2 \equiv \frac{u(e_s^{\text{calc}})^2}{e_s^2} + \frac{u(e_c^{\text{calc}})^2}{e_c^2} \quad \text{and} \quad \text{A19)}$$

$$u_r(\Delta f^{\text{calc}})^2 \equiv \frac{u(f_s^{\text{calc}})^2}{f_s^2} + \frac{u(f_c^{\text{calc}})^2}{f_c^2}. \quad \text{A20)}$$

3. Relative Humidity When the Generator is Used in 2-P Mode or 1-P Mode

Here we consider the total uncertainty for the relative humidity RH in a chamber with temperature T_c , pressure P_c when the generator is used in 2-P or 1-P mode. By the WMO definition, the relative humidity is defined as

$$RH \equiv \frac{x}{x_c} = \frac{e_p}{e_c f_c}, \quad \text{A21)}$$

where x_c is the water amount fraction in the chamber at saturation and the partial water vapor pressure e_p in the chamber is given by

$$e_p = x P_c \quad \text{A22)}$$

and e_c is the saturated water vapor pressure at temperature T_c . Note that e_c is a function of T_c , while e_p is an independent variable. Placing Eq. A22 into Eq. A21,

$$RH \equiv \frac{x P_c}{e_c f_c} = \frac{e_s f_s P_c}{e_c f_c P_s}, \quad \text{A23)}$$

The total uncertainty for this case is obtained by applying Eq. A2 to Eq. A22, which yields

$$d(RH) = \frac{f_s P_c}{e_c f_c P_s} de_s + \frac{e_s P_c}{e_c f_c P_s} df_s + \frac{e_s f_s}{e_c f_c P_s} dP_c - \frac{e_s f_s P_c}{e_c f_c^2 P_s} df_c - \frac{e_s f_s P_c}{e_c f_c P_s^2} dP_s - \frac{e_s f_s P_c}{e_c^2 f_c P_s} de_c. \quad \text{A24)}$$

Recognizing that

$$de = de^{\text{calc}} + \frac{de}{dT} dT, \quad \text{A25)}$$

A24 becomes

$$d(RH) = \frac{P_c f_s}{P_s e_c f_c} \left[de_s^{\text{calc}} + \frac{de_s}{dT_s} dT_s \right] + \frac{e_s P_c}{P_s e_c f_c} df_s + \frac{e_s f_s}{P_s e_c f_c} dP_c - \frac{e_s P_c f_s}{e_c P_s f_c^2} df_c - \frac{e_s P_c f_s}{e_c P_s^2 f_c} dP_s - \frac{e_s P_c f_s}{e_c^2 P_s f_c} \left[de_c^{\text{calc}} + \frac{de_c}{dT_c} dT_c \right]. \quad \text{A26)}$$

Inserting Eqs. A14 and A15 yields:

$$\begin{aligned}
 d(RH) &= \frac{P_c f_s}{P_s e_c f_c} \frac{de_s}{dT_s} dT_s + \frac{e_s f_s}{P_s e_c f_c} dP_c - \frac{e_s f_s P_c}{e_c f_c P_s^2} dP_s - \frac{e_s f_s P_c}{e_c^2 f_c P_s} \frac{de_c}{dT_c} dT_c \\
 &\quad + \frac{e_s f_s P_c}{e_c f_c P_s} \frac{de_c}{dT_c} d\Delta e^{\text{calc}} + \frac{e_s f_s P_c}{e_c f_c P_s} d\Delta f
 \end{aligned} \tag{A27}$$

$$= \frac{P_c e_s f_s}{P_s e_c f_c} \left[\frac{1}{e_s} \frac{de_s}{dT_s} dT_s + \frac{dP_c}{P_c} - \frac{dP_s}{P_s} - \frac{1}{e_c} \frac{de_c}{dT_c} dT_c + d\Delta e^{\text{calc}} + d\Delta f \right]$$

Noting Eq. A23, the standard relative uncertainty for the relative humidity is then

$$\begin{aligned}
 u_r(RH)^2 &= \left[\frac{u(RH)}{RH} \right]^2 = \left[\left(\frac{1}{e_s} \frac{de_s}{dT_s} \right)^2 u(T_s)^2 + \frac{1}{P_s^2} u(P_s)^2 + \left(\frac{1}{e_c} \frac{de_c}{dT_c} \right)^2 u(T_c)^2 + \frac{1}{P_c^2} u(P_c)^2 \right. \\
 &\quad \left. + u_r(\Delta e^{\text{calc}}) + u_r(\Delta f^{\text{calc}}) \right]
 \end{aligned} \tag{A28}$$

Once again, the values of $u_r(\Delta e^{\text{calc}})$ and $u_r(\Delta f^{\text{calc}})$ are best estimated by Eq. A16 when the generator is used in 1-P mode and by Eq. A17 and Eq. A18 when the generator is used in 2-P mode.

4. Water Amount Fraction When the Generator is Used in Divided-flow Mode

For the generator used with the divided-flow method, the differential for the amount fraction may be expanded as

$$dx = \frac{\dot{n}_s dx_s + \dot{n}_p dx_p}{\dot{N}} + \frac{\dot{n}_p (x_s - x_p)}{\dot{N}^2} d\dot{n}_s - \frac{\dot{n}_s (x_s - x_p)}{\dot{N}^2} d\dot{n}_p \tag{A29}$$

Since $x_p \ll x_s$, this reduces to

$$dx \cong \frac{\dot{n}_s}{\dot{N}} dx_s + \frac{\dot{n}_p}{\dot{N}} dx_p + \frac{\dot{n}_p x_s}{\dot{N}^2} d\dot{n}_s - \frac{\dot{n}_s x_s}{\dot{N}^2} d\dot{n}_p \tag{A30}$$

Using the result of Eq. A6 as dx_s , and noting $x_s = e_s f_s / P_s$, this becomes

$$dx \cong \frac{\dot{n}_s f_s}{\dot{N} P_s} \frac{de_s}{dT_s} dT_s - \frac{\dot{n}_s e_s f_s}{\dot{N} P_s^2} dP_s + \frac{\dot{n}_s f_s}{\dot{N} P_s} de_s^{\text{calc}} + \frac{\dot{n}_s e_s}{\dot{N} P_s} df_s^{\text{calc}} + \frac{\dot{n}_p}{\dot{N}} dx_p + \frac{\dot{n}_p e_s f_s}{\dot{N}^2 P_s} d\dot{n}_s - \frac{\dot{n}_s e_s f_s}{\dot{N}^2 P_s} d\dot{n}_p \tag{A31}$$

Noting that $x \cong \dot{n}_s e_s f_s / \dot{N} P_s$ and $x_s = e_s f_s / P_s$, the amount fraction standard relative uncertainty $u_r(x)$ is then given by

$$u_r(x)^2 = \left[\frac{u(x)}{x} \right]^2 \cong \left(\frac{1}{e_s} \frac{de_s}{dT_s} \right)^2 u(T_s)^2 + \frac{u(P_s)^2}{P_s^2} + \frac{u(e_s^{\text{calc}})^2}{e_s^2} + \frac{u(f_s^{\text{calc}})^2}{f_s^2} + \frac{u(\dot{n}_p)^2}{\dot{N}^2} + \left(\frac{x_s}{x} - 1 \right)^2 \left(\frac{u(x_p)^2}{x_s^2} + \frac{u(\dot{n}_s)^2}{\dot{N}^2} \right) \quad \text{A32)}$$

5. Frost-point Temperature When the Generator is Used in Divided-flow Mode

In the hybrid generator, the divided-flow method will only be used for generating frost points. We expand the frost-point temperature differential by combining Eqs. A11 and A31, which yields

$$dT_{\text{FP}} = \frac{P_c}{[de_c/dT_c]f_c} \left[\frac{\dot{n}_s f_s}{\dot{N} P_s} \frac{de_s}{dT_s} dT_s - \frac{\dot{n}_s e_s f_s}{\dot{N} P_s^2} dP_s + \frac{\dot{n}_s f_s}{\dot{N} P_s} de_s^{\text{calc}} + \frac{\dot{n}_s e_s}{\dot{N} P_s} df_s^{\text{calc}} + \frac{\dot{n}_p}{\dot{N}} dx_p + \frac{\dot{n}_p e_s f_s}{\dot{N}^2 P_s} d\dot{n}_s + \frac{\dot{n}_s e_s f_s}{\dot{N}^2 P_s} d\dot{n}_p + \frac{x}{P_c} dP_c - \frac{x}{f_c} df_c^{\text{calc}} - \frac{f_c}{P_c} de_c^{\text{calc}} \right] \quad \text{A33)}$$

Here e_c is the saturated vapor pressure for ice. Because of this, we assume no correlation between the uncertainties of e_c^{calc} and e_s^{calc} , since e_s^{calc} is the calculation of the saturated vapor pressure for water and is different for that of ice. Using the definitions for $d\Delta e^{\text{calc}}$ and $d\Delta f^{\text{calc}}$ in Eqs. A14-A15, and noting that $x = \dot{n}_s e_s f_s / \dot{N} P_s = e_c f_c / P_c$ and $x_s = e_s f_s / P_s$, Eq. A33 becomes

$$dT_{\text{FP}} = \frac{e_c}{[de_c/dT_c]} \left[\frac{1}{e_s} \frac{de_s}{dT_s} dT_s - \frac{dP_s}{P_s} + \frac{dP_c}{P_c} + d\Delta e^{\text{calc}} + d\Delta f^{\text{calc}} + \left(\frac{x_s}{x} - 1 \right) \left(\frac{dx_p}{x_s} + \frac{d\dot{n}_s}{\dot{N}} \right) + \frac{d\dot{n}_p}{\dot{N}} \right] \quad \text{A34)}$$

The frost-point temperature uncertainty then becomes

$$u(T_{\text{FP}})^2 = \frac{e_c^2}{[de_c/dT_c]^2} \left[\left(\frac{1}{e_s} \frac{de_s}{dT_s} \right)^2 u(T_s)^2 + \frac{u(P_s)^2}{P_s^2} + \frac{u(P_c)^2}{P_c^2} + u_r(\Delta e^{\text{calc}})^2 + u_r(\Delta f^{\text{calc}})^2 + \left(\frac{x_s}{x} - 1 \right)^2 \left(\frac{u(x_p)^2}{x_s^2} + \frac{u(\dot{n}_s)^2}{\dot{N}^2} \right) + \frac{u(\dot{n}_p)^2}{\dot{N}^2} \right] \quad \text{A35)}$$

Here, we once again use the conventional method for estimating $u_r(\Delta e^{\text{calc}})^2$ and $u_r(\Delta f^{\text{calc}})^2$, which employs Eq. A19-A20.

6. Relative Humidity When the Generator is Used in Divided-flow Mode

Here we consider the total uncertainty for the relative humidity RH in a chamber with temperature T_c and pressure P_c when the generator is used in divided-flow mode. From Eqs. A21-A23, the relative humidity is

$$RH \equiv \frac{xP_c}{e_c f_c}, \quad \text{A36)}$$

and so

$$d(RH) = \frac{P_c}{e_c f_c} dx + \frac{x}{e_c f_c} dP_c - \frac{xP_c}{e_c^2 f_c} de_c - \frac{xP_c}{e_c f_c^2} df_c \quad \text{A37)}$$

Inserting Eq. 6, Eq. A25, and Eq. A31 and into Eq. A37 yields:

$$d(RH) = \frac{xP_c}{e_c f_c} \left[\frac{1}{e_s} \frac{de_s}{dT_s} dT_s - \frac{dP_s}{P_s} + \frac{de_s^{\text{calc}}}{e_s} + \frac{df_s^{\text{calc}}}{f_s} + \left(\frac{x_s}{x} - 1 \right) \left(\frac{dx_p}{x_s} + \frac{d\dot{n}_s}{\dot{N}} \right) - \frac{d\dot{n}_p}{\dot{N}} \right] \\ + \left(\frac{P_c}{e_c f_c} \right) \left(x + \frac{\dot{n}_p}{\dot{N}} x_p \right) \left(\frac{dP_c}{P_c} - \frac{1}{e_c} \frac{de_c}{dT_c} dT_c - \frac{de_c^{\text{calc}}}{e_c} - \frac{df_c^{\text{calc}}}{f_c} \right) \quad \text{A38)}$$

Noting that $x_p \cong 0$ and using Eqs. A14 and A15, this can be arranged to be

$$d(RH) = \frac{xP_c}{e_c f_c} \left[\frac{1}{e_s} \frac{de_s}{dT_s} dT_s - \frac{dP_s}{P_s} - \frac{1}{e_c} \frac{de_c}{dT_c} dT_c + \frac{dP_c}{P_c} + d\Delta e^{\text{calc}} + d\Delta f^{\text{calc}} \right. \\ \left. + \left(\frac{x_s}{x} - 1 \right) \left(\frac{dx_p}{x_s} + \frac{d\dot{n}_s}{\dot{N}} \right) - \frac{d\dot{n}_p}{\dot{N}} \right] \quad \text{A38)}$$

The relative uncertainty for the relative humidity is then:

$$u_r(RH) = \left[\frac{u(RH)}{RH} \right]^2 = \left[\left(\frac{1}{e_s} \frac{de_s}{dT_s} \right)^2 u(T_s)^2 + \frac{u(P_s)^2}{P_s^2} + \left(\frac{1}{e_c} \frac{de_c}{dT_c} \right)^2 u(T_c)^2 + \frac{u(P_c)^2}{P_c^2} + u_r(\Delta e^{\text{calc}}) + u_r(\Delta f^{\text{calc}}) + \left(\frac{x_s}{x} - 1 \right)^2 \left(\frac{u(x_p)^2}{x_s^2} + \frac{u(\dot{n}_s)^2}{\dot{N}^2} \right) + \frac{u(\dot{n}_p)^2}{\dot{N}^2} \right]^2, \quad \text{A39)}$$

where $u_r(\Delta e^{\text{calc}})^2$ and $u_r(\Delta f^{\text{calc}})^2$ are given by Eq. A19-A20. Note that in the limit of $x = x_s$, Eq. A39 is equivalent to Eq. A28.

Appendix II. Uncertainty Element Subcomponents for the HHG and its Test Chamber

Table 5. Subcomponents for the uncertainty elements T_s , T_c , P_s , and P_c for the Hybrid Generator and its Test Chamber. Note that saturation efficiency, air contamination, and water contamination have been assigned to be subcomponents of T_s for simplicity.

	Source of uncertainty		Standard Uncertainty	Unit
Saturator Temperature T_s	<i>SPRT</i>	Calibration	0.5	mK
		Drift	0.3	mK
		Self-heating	0.1	mK
	<i>Bridge</i>	Calibration	0.1	mK
		Resolution	0.1	mK
	<i>Saturator</i>	Temperature gradients	1 ($T \leq 40^\circ\text{C}$) 0.16T/°C – 5.4 ($T > 40^\circ\text{C}$)	mK
		Temperature Stability	1	mK
	<i>Other</i>	Saturation efficiency	0.5	mK
		Air contamination	< 0.2	mK
		Water contamination	< 0.2	mK
Chamber Temperature T_c	<i>PRT</i>	Calibration	10	mK
		Drift	0.3	mK
		Self-heating	0.1	mK
	<i>Bridge</i>	Calibration	0.1	mK
		Resolution	0.1	mK
	<i>Chamber</i>	Temperature Nonuniformity	10	mK
	Saturator Pressure P_s	<i>Pressure gauge</i>	Calibration	7
Drift			10 + 0.0001 P_s /Pa	Pa
Resolution			7	Pa
Hydrostatic head			1	Pa
Flow effect			2	Pa
Repeatability			7	Pa
<i>Saturator</i>		P_s stability	7 ($P_s \approx$ ambient pressure) 20 ($P_s >$ ambient pressure)	Pa
Chamber Pressure P_c		<i>Pressure gauge</i>	Calibration	7
	Drift		5	Pa
	Resolution		7	Pa
	Hydrostatic head		1	Pa
	Flow effect		2	Pa
	Repeatability		7	Pa
	<i>Chamber</i>	P_c stability	7	Pa

Appendix III. Sample Calibration Reports

Order No: O-0000009876
 Service ID: 36070S
 Date: August 6, 2021

RH Systems Dew Point Mirror RH-473-RP2, S/N 12-3456

Table 1
 Dew/Frost Point Temperature

Pt.	Calibration Values		Calibration Uncertainties		
	NIST T_{DP}, T_{FP} (°C)	DUT T_{DP}, T_{FP} (°C)	NIST $U(T_{DP}, T_{FP})$ (°C)	DUT $U(T_{DP}, T_{FP})$ (°C)	U_{Tot} ($k=2$) (°C)
1	20.72	20.63	0.02	0.05	0.05
2	17.79	17.73	0.02	0.05	0.05
3	13.02	12.95	0.02	0.05	0.05
4	6.20	6.19	0.02	0.05	0.05
5	-8.38	-8.36	0.02	0.05	0.05
6	15.38	15.32	0.02	0.05	0.05
7	10.65	10.61	0.02	0.05	0.05

In this table,

NIST T_{DP} is the dew point temperature generated by the NIST hybrid humidity generator,
 NIST T_{FP} is the frost point temperature generated by the NIST hybrid humidity generator

DUT T_{DP} is the dew point temperature measured by the device under test,
 DUT T_{FP} is the frost point temperature measured by the device under test,

NIST $U(T_{DP}, T_{FP})$ is the expanded uncertainty ($k=2$) of the hybrid humidity generator,
 DUT $U(T_{DP}, T_{FP})$ is the estimated expanded uncertainty ($k=2$) of the device under test, based on its specifications,
 and

U_{Tot} is the total expanded uncertainty ($k=2$) of the calibration, as calculated from $U(T_{DP, NIST})$ and $U(T_{DP, DUT})$.

Note: the values above 0 °C are dew point temperatures and the values below 0 °C are frost point temperatures.

RH Systems Dew Point Mirror RH-473-RP2, S/N 12-3456

Table 2
 External Thermometer Temperature T

Pt.	Calibration Values		Calibration Uncertainties		
	T_{NIST} (°C)	T_{DUT} (°C)	$U(T_{\text{NIST}})$ ($k=2$) (°C)	$U(T_{\text{DUT}})$ ($k=2$) (°C)	$U_{\text{Tot}}(T)$ ($k=2$) (°C)
1	22.41	22.42	0.01	0.01	0.01
2	22.30	22.31	0.01	0.01	0.01
3	22.41	22.42	0.01	0.01	0.01
4	22.39	22.40	0.01	0.01	0.01
5	23.23	23.25	0.01	0.01	0.01
6	24.85	24.86	0.01	0.01	0.01
7	19.94	19.95	0.01	0.01	0.01

In this table,

T_{NIST} is the bath temperature as measured by the NIST reference thermometer,

T_{DUT} is the bath temperature as measured by the DUT external thermometer,

$U(T_{\text{NIST}})$ is the expanded uncertainty ($k=2$) of the NIST calibration,

$U(T_{\text{DUT}})$ is the estimated expanded uncertainty ($k=2$) of T_{DUT} , based on the reproducibility of similar probes, and

U_{Tot} is the total expanded uncertainty ($k=2$) of the external thermometer calibration, as calculated from $U(T_{\text{NIST}})$ and $U(T_{\text{DUT}})$.

RH Systems Dew Point Mirror RH-473-RP2, S/N 12-3456

Table 3
 Relative Humidity

Pt.	Calibration Values		Calibration Uncertainties		
	RH_{NIST} (%)	RH_{DUT} (%)	$U(RH_{NIST})$ ($k=2$) (%)	$U(RH_{DUT})$ ($k=2$) (%)	$U_{Tot}(RH)$ ($k=2$) (%)
1	90.2	89.6	0.1	0.2	0.2
2	75.6	75.3	0.1	0.2	0.2
3	55.3	55.0	0.1	0.1	0.1
4	35.0	34.9	0.1	0.1	0.1
5	10.5	10.5	0.1	0.1	0.1
6	55.6	55.4	0.1	0.1	0.1
7	55.0	54.8	0.1	0.1	0.1

For each point in this table,

RH_{NIST} is the is the calculated relative humidity of a sample of air with the dew point generated by the HHG (given for this point in Table 1) and at the temperature measured by the NIST thermometer (given for this point in Table 2),

RH_{DUT} is the relative humidity measured by the DUT, determined from the measured dew point (given for this point in table 1) and measured external thermometer temperature (given for this point in Table 2),

$U(RH_{NIST})$ is the expanded uncertainty ($k=2$) of the NIST calibration, excluding DUT uncertainties,

$U(RH_{DUT})$ is the estimated expanded uncertainty ($k=2$) of RH_{DUT} due to reproducibility, based on its specifications, and

$U(RH_{Tot})$ is the total expanded uncertainty ($k=2$) of the relative-humidity calibration, as calculated from $U(RH_{NIST})$ and $U(RH_{DUT})$.

U_{Tot} is the total expanded uncertainty ($k=2$) of the relative humidity calibration, as calculated from $U(RH_{NIST})$ and $U(RH_{DUT})$.



UNITED STATES DEPARTMENT OF COMMERCE
National Institute of Standards and Technology
Gaithersburg, Maryland 20899-8361

Sample Calibration Report

REPORT OF CALIBRATION

THERMOHYGROMETER

Fluke Model 1620 “DewK” Thermohygrometer, S/N 12345 with
Fluke Thermo-hygrometer Sensor 2626-S, S/N 98765

Submitted
by
DPM, Inc.
Somewhere, NC 98765

The thermohygrometer was calibrated by comparison against air of known water vapor content, pressure and temperature. The moist air was generated by the NIST Hybrid Humidity Generator (HHG) and channeled through stainless-steel tubes into a temperature-controlled stainless-steel test chamber. Before entering the chamber, the moist air was directed through a heat exchanger to bring it to the temperature of the chamber. The flowing air exited the test chamber through a 122 cm long stainless-steel tube. The following procedure was used for the calibration of the device under test (DUT). The generator was set to produce humidified air with a flow rate of 150 standard liters per minute (SLM) through the chamber. The moisture content in the chamber was measured by a NIST dew-point hygrometer. Once the flow started, humidity measurements were made with the hygrometers to determine when the readings reached a steady state. For each calibration point, once a steady state was reached, the determined values of the generated relative humidity were averaged over a minimum of 30 minutes, as were the values of the humidity from the customer hygrometer. These average values are presented below in Table 1 for all calibration points. The relative humidity standards generated by the HHG are traceable to the International System of Units (SI) through NIST pressure and temperature standards. The generator and the complete calibration procedure are described in NIST SP250-83r1, entitled “Calibration of Hygrometers with the Hybrid Humidity Generator”, which may be found at <https://nvlpubs.nist.gov/nistpubs/Legacy/SP/nistspecialpublication250-83r1.pdf>. The results in this report pertain only to the item tested.

In Table 1, three uncertainty values are provided for each calibration point. $U(T_{\text{NIST}})$ and $U(RH_{\text{NIST}})$ are the expanded uncertainties of the NIST-determined values of the temperature and relative humidity, respectively. $U(T_{\text{DUT}})$ and $U(RH_{\text{DUT}})$ are the expanded reproducibility-related uncertainties of the DUT measurements of the temperature and relative humidity, respectively; these uncertainties are estimated using the manufacturer specifications of the hygrometer. Finally, $U_{\text{Tot}}(T)$ and $U_{\text{Tot}}(RH)$ are the total expanded uncertainties of the temperature and relative-humidity calibrations, respectively, obtained by adding U_{HHG} and U_{DUT} in quadrature. An expanded uncertainty is expressed as $U = ku_c$, with U determined from a combined standard uncertainty u_c and a coverage factor $k = 2$. The values of $U(T_{\text{NIST}})$ and $U(RH_{\text{NIST}})$ are dependent on the uncertainties of individual parameters for the HHG and test chamber. A discussion of the uncertainty components for the HHG uncertainties as a function of the generator parameters is provided in NIST SP 250-83r1.

For the Director
National Institute of Standards and Technology

Julia Scherschligt
Leader, Thermodynamic Metrology Group
Sensor Science Division

Measurement and analysis performed by Christopher Meyer
Test Number: 0000009876
Service ID: 36070S
Purchase Order Number: 12345
Measurements performed: 7/27/21-8/01/21
Report Date: August 6, 2021

Page 1 of 2

Table 1

Fluke Model 1620 “DewK” Thermohygrometer, S/N 12345 with
 Fluke Thermo-hygrometer Sensor 2626-S, S/N 98765

a. Test Chamber Temperature T

Pt.	Calibration Values		Calibration Uncertainties		
	T_{NIST} (°C)	T_{DUT} (°C)	$U(T_{NIST})$ ($k=2$) (°C)	$U(T_{DUT})$ ($k=2$) (°C)	$U_{Tot}(T)$ ($k=2$) (°C)
1	22.96	22.87	0.03	0.025	0.04
2	22.99	22.91	0.03	0.025	0.04
3	22.98	22.89	0.03	0.025	0.04
4	19.04	18.95	0.03	0.025	0.04
5	29.00	28.91	0.03	0.025	0.04

b. Test Chamber Relative Humidity RH

Pt.	Calibration Values		Calibration Uncertainties		
	RH_{NIST} (%)	RH_{DUT} (%)	$U(RH_{NIST})$ ($k=2$) (%)	$U(RH_{DUT})$ ($k=2$) (%)	$U_{Tot}(RH)$ ($k=2$) (%)
1	84.0	84.5	0.4	1.0	1.1
2	50.0	50.4	0.4	1.0	1.1
3	17.6	18.8	0.4	1.0	1.1
4	49.6	50.7	0.4	1.0	1.1
5	49.9	50.1	0.4	1.0	1.1

In this table,

T_{NIST} is the test chamber temperature, as measured by the NIST reference thermometer,
 T_{DUT} is the test chamber temperature, as measured by the device under test,
 $U(T_{NIST})$ is the expanded uncertainty ($k=2$) of temperature inside the test chamber,
 $U(T_{DUT})$ is the estimated expanded uncertainty ($k=2$) of the DUT for temperature measurement due to reproducibility,
 based on its specifications, and
 $U(T_{Tot})$ is the total expanded uncertainty ($k=2$) of the temperature calibration, as calculated from $U(T_{NIST})$ and $U(T_{DUT})$.

RH_{NIST} is the relative humidity in the HHG test chamber, calculated using the chamber temperature and the known
 moisture content generated by the HHG into the chamber

RH_{DUT} is the relative humidity in the HHG test chamber, as measured by the device under test

$U(RH_{NIST})$ is the expanded uncertainty ($k=2$) of relative humidity inside the test chamber,

$U(RH_{DUT})$ is the estimated expanded uncertainty ($k=2$) of the DUT for relative-humidity measurement due to
 reproducibility, based on its specifications, and

$U(RH_{Tot})$ is the total expanded uncertainty ($k=2$) of the relative-humidity calibration, as calculated from $U(RH_{NIST})$ and
 $U(RH_{DUT})$.



Sample Calibration Report

REPORT OF CALIBRATION

CAVITY RING DOWN HYGROMETER

Tiger Optics, Model LaserTrace 3 H₂O

S/N 12345

Submitted

by

DPM, Inc.

Somewhere, NC 98765

The cavity ring down hygrometer was calibrated by comparison against air of known water vapor content, generated by the NIST Hybrid Humidity Generator (HHG). The outlet from the generator was connected to the inlet of the hygrometer using stainless steel tubing. The pressure at the inlet of the hygrometer was slightly above ambient pressure. The outlet of the hygrometer was attached to a diaphragm pump. The water amount fraction generated during the calibration ranged from 0.5 micromol/mol to 5.0 micromol/mol. For each calibration point, the following procedure was used. The generator was set to produce humidified air with a flow rate of 17 standard liters per minute (SLM), this air passed in parallel through the test hygrometer, a check hygrometer, and a bypass port. Before measurements were made, the hygrometer was configured for air as the carrier gas and the hygrometer was autotuned. Once the flow started, humidity measurements were made with the hygrometer to determine when the readings reached a steady state. Once a steady state was reached, the determined values of the generated humidity were averaged over a minimum of 30 minutes, as were the values of the humidity from the hygrometer. The hygrometer values were read and recorded from the display. These average values are presented below in Table 1 for all calibration points. The relative humidity standards generated by the HHG are traceable to the International System of Units (SI) through NIST pressure and temperature standards. The generator and the complete calibration procedure are described in NIST SP250-83r1, entitled "Calibration of Hygrometers with the Hybrid Humidity Generator", which may be found at <https://nvlpubs.nist.gov/nistpubs/Legacy/SP/nistspecialpublication250-83r1.pdf>. The results in this report pertain only to the item tested.

In Table 1, three uncertainty values are provided for each calibration point. U_{HHG} is the expanded uncertainty of the water amount fraction generated by the NIST Hybrid Humidity Generator. U_{DUT} is the expanded uncertainty of the device under test due to reproducibility, estimated by the manufacturer. Finally, U_{Tot} is the total expanded uncertainty of the calibration, obtained by adding U_{HHG} and U_{DUT} in quadrature. An expanded uncertainty is expressed as $U = ku_c$, with U determined from a combined standard uncertainty u_c and a coverage factor $k = 2$. The values of U_{HHG} are dependent on the uncertainties of individual generator parameters. A discussion and presentation of the total HHG uncertainties and their components as a function of the generator parameters are provided in NIST SP 250-83r1.

For the Director
National Institute of Standards and Technology

Julia Scherschligt
Group Leader, Thermodynamic Metrology
Sensor Science Division

Measurement and analysis performed by Christopher Meyer

Order Number: 0000009876

Service ID: 36070S

Measurements performed: August 4, 2021

Report Date: August 6, 2021

Order No: 000009876
 Service ID: 36070S
 Date: August 6, 2021

This publication is available free of charge from: <https://doi.org/10.6028/NIST.SP.250-831>

Table 1

Tiger Optics Cavity Ring Down Hygrometer
 LaserTrace 3 H₂O; S/N 12345

Calibration Values		Calibration Uncertainties		
NIST HHG x (micromol/mol)	DUT x (micromol/mol)	U_{HHG} ($k=2$) (micromol/mol)	U_{DUT} ($k=2$) (micromol/mol)	U_{Tot} ($k=2$) (micromol/mol)
5.059	5.149	0.01	0.05	0.05
1.039	1.048	0.003	0.01	0.01
0.511	0.517	0.002	0.005	0.005

In this table,

NIST HHG x is the water amount fraction generated by the NIST hybrid humidity generator,

DUT x is the water amount fraction measured by the device under test,

U_{HHG} is the expanded uncertainty ($k=2$) of the hybrid humidity generator,

U_{DUT} is the estimated expanded uncertainty ($k=2$) of the device under test, based on its specifications, and

U_{Tot} is the total expanded uncertainty ($k=2$) of the calibration, as calculated from U_{HHG} and U_{DUT} .



National Institute of Standards and Technology
 Technology Administration, U.S. Department of Commerce